Les Cahiers du GERAD ISSN: 0711–2440

Modeling and solving the traveling salesman problem with speed optimization for a plug-in hybrid electric vehicle

F. Wu, Y. Adulyasak, J.-F. Cordeau

G–2023–42

September 2023

Citation suggérée : F. Wu, Y. Adulyasak, J.-F. Cordeau (Septembre 2023). Modeling and solving the traveling salesman problem with speed optimization for a plug-in hybrid electric vehicle, Rapport technique, Les Cahiers du GERAD G– 2023–42, GERAD, HEC Montréal, Canada.

Avant de citer ce rapport technique, veuillez visiter notre site Web (https://www.gerad.ca/fr/papers/G-2023-42) afin de mettre à jour vos données de référence, s'il a été publié dans une revue scientifique.

Suggested citation: F. Wu, Y. Adulyasak, J.-F. Cordeau (September 2023). Modeling and solving the traveling salesman problem with speed optimization for a plug-in hybrid electric vehicle, Technical report, Les Cahiers du GERAD G–2023–42, GERAD, HEC Montréal, Canada.

Before citing this technical report, please visit our website (https://www.gerad.ca/en/papers/G-2023-42) to update your reference data, if it has been published in a scientific journal.

La publication de ces rapports de recherche est rendue possible grâce au soutien de HEC Montréal, Polytechnique Montréal, Université McGill, Université du Québec à Montréal, ainsi que du Fonds de recherche du Québec – Nature et technologies.

Dépôt légal – Bibliothèque et Archives nationales du Québec, 2023
– Bibliothèque et Archives Canada, 2023

The publication of these research reports is made possible thanks to the support of HEC Montréal, Polytechnique Montréal, McGill University, Université du Québec à Montréal, as well as the Fonds de recherche du Québec – Nature et technologies.

Legal deposit – Bibliothèque et Archives nationales du Québec, 2023
– Library and Archives Canada, 2023

GERAD HEC Montréal
3000, chemin de la Côte-Sainte-Catherine
Montréal (Québec) Canada H3T 2A7

Tél. : 514 340-6053
Téléc. : 514 340-5665
info@gerad.ca
www.gerad.ca

Modeling and solving the traveling salesman problem with speed optimization for a plug-in hybrid electric vehicle

Fuliang Wu [a, b]

Yossiri Adulyasak [a, b]

Jean-François Cordeau [a, b]

[a] *GERAD, Montréal (Qc), Canada, H3T 1J4*

[b] *HEC Montréal, Montréal (Qc), Canada, H3T 2A7*

fuliang.w@outlook.com
yossiri.adulyasak@hec.ca
jean-francois.cordeau@hec.ca

September 2023
Les Cahiers du GERAD
G–2023–42

Abstract : This paper investigates a variant of the traveling salesman problem (TSP) with speed optimization for a plug-in hybrid electric vehicle (PHEV), simultaneously optimizing the average speed and operation mode for each road segment in the route. Two mixed-integer nonlinear programming models are proposed for the problem: one with continuous speed decision variables and one with discretized variables. Since the models are non-linear, we propose reformulation schemes and introduce valid inequalities to strengthen them. We also describe a branch-and-cut algorithm to solve these reformulations. Extensive numerical experiments are performed to demonstrate the algorithm's performance in terms of computing time and energy consumption costs. Specifically, the proposed solution method can efficiently solve instances with a realistic number of customers and outperforms the benchmark approaches from the literature. Integrating speed optimization into the TSP of a PHEV can lead to significant energy savings compared to the fixed-speed TSP. In addition, the proposed model is extended to investigate the impact of the presence of charging stations, which makes the problem harder to solve but has the potential to further reduce energy consumption costs.

Keywords : plug-in hybrid electric vehicle, traveling salesman problem, speed optimization, branch-and-cut

Acknowledgements: The authors are grateful to Christian Doppstadt, Achim Koberstein, and Daniele Vigo for generously providing their instances, which were used in our computational experiments.

1 Introduction

Reducing emissions is a key focus of international climate change agreements due to the recognized role of greenhouse gases in causing global temperature rises (Bektaş et al. 2019). Vehicle electrification has emerged as an effective strategy for reducing emissions from road transportation. In line with this effort, the United Parcel Service (UPS), a prominent delivery company, aims to incorporate more than 1000 electric and plug-in hybrid electric vehicles into its fleet by 2025 (UPS 2022). In Canada, the sales of plug-in hybrid electric vehicles (PHEVs) have surged by 95 percent since 2020, reaching approximately 28,300 units in 2021 (Carlier 2022). Electric vehicles encompass pure battery electric vehicles (BEVs) and PHEVs, with the latter drawing power from both battery and fuel sources. Notably, PHEVs typically have larger battery capacities and can recharge their batteries from an external electrical outlet, which differs from standard hybrid electric vehicles (HEVs) (Sioshansi 2012).

PHEVs commonly utilize an internal combustion engine (ICE) and an electric machine (EM) as their two power sources. Two main types of PHEVs are defined according to their powertrain configuration: series and parallel. In a series configuration, only the EM is connected to the wheels, with the ICE being utilized solely to generate electricity. On the contrary, the parallel configuration connects both the ICE and EM to the wheels, enabling the vehicle to operate using one or both power sources. This paper focuses on PHEVs with a parallel configuration, which offers greater operational flexibility but also presents routing challenges arising from the requirement to determine optimal operation modes (Nejad et al. 2017).

Most of the previous studies on HEV and PHEV routing problems assume that the cost on each road segment is given (e.g., Bahrami et al. 2020; Doppstadt, Koberstein, and Vigo 2016, 2020; Nejad et al. 2017), but vehicle energy consumption highly depends on the driving speed (Bektaş and Laporte 2011; Demir, Bektaş, and Laporte 2014; Fukasawa et al. 2018; Wu et al. 2021). Thus, this paper aims to model and solve a traveling salesman problem (TSP) with speed optimization for a PHEV, which is referred to as PHEV-TSPS. The objective of the PHEV-TSPS is to minimize a PHEV's energy consumption cost over a TSP, which involves deciding both the service sequence of the customers and vehicle's operation mode (e.g., pure ICE, pure EM, or both EM and ICE) on each road segment. In short, the PHEV-TSPS jointly optimizes the visiting sequence of the customers, the operation mode on each arc, and the average driving speed on each arc.

The PHEV-TSPS is a challenging problem to solve because it is an extension of the TSP and is thus NP-hard (Papadimitriou 1977). The multiple operation modes of PHEVs make the resulting TSP more complex, as the underlying graph becomes a multigraph with a significantly increased number of possible solutions. For example, as reported in Doppstadt, Koberstein, and Vigo (2016), even with a state-of-the-art solver such as Cplex, it took nearly 95 hours to find an optimal solution for an HEV TSP instance with only 10 customers. Although the heuristic that they propose is faster, it still requires considerable time (hours) to find high-quality solutions for instances with 50 customers. Furthermore, incorporating speed optimization makes the problem even more difficult because the energy consumption model is nonlinear. The primary goal of this study is to propose an exact algorithm that can solve the problem with a realistic number of customers within a reasonable time.

This paper contributes to the existing literature in the following ways. First, it enhances the accuracy of energy consumption evaluation by incorporating speed optimization into the PHEV TSP and develops two mixed-integer nonlinear programming models for the PHEV-TSPS. In addition, we prove that the integration of speed optimization in the PHEV TSP can yield energy consumption cost savings. Second, this paper proposes valid inequalities for the models and embeds them into a branch-and-cut algorithm, enabling the problem with a realistic number of customers to be solved efficiently. Third, the paper evaluates the performance of the proposed methods through extensive computation experiments, considering computational efficiency and energy consumption costs. The proposed solution methods are capable of efficiently solving instances with up to 70 customers to optimality and are flexible enough to be applied to the HEV TSP previously studied in the literature. In particular, our exact algorithm can find optimal solutions to benchmark instances in smaller computing time than those used by the heuristic of Doppstadt, Koberstein, and Vigo (2016). In addition, the integration of speed optimization can result in significant savings in energy consumption costs compared to the fixed-speed TSP. Fourth and last, to ensure reproducibility and facilitate knowledge dissemination, we have made our code and instances publicly available.

The remainder of the paper is structured as follows. Section 2 provides a brief review of the relevant literature. Section 3 presents a formal definition of the PHEV-TSPS and formulates the associated mixed-integer nonlinear programming model. In Section 4, several valid inequalities for the proposed model are introduced. Section 5 outlines the customized branch-and-cut algorithm designed for solving the PHEV-TSPS. Section 6 presents computational experiments to evaluate the proposed methods. Finally, Section 7 concludes the paper.

2 Literature review

Vehicle electrification represents a significant step towards achieving environmental sustainability, and electric vehicles can be classified into three main categories: BEVs powered solely by EMs, HEVs, and PHEVs. This section will briefly review the routing problems associated with each category.

Careful route planning can help alleviate the range anxiety experienced by BEV drivers, which arises from the limited battery capacity. The routing problems of BEVs have been extensively studied in the existing literature and typically offer two options to address this issue. The first option is to allow BEVs to stop at charging stations along the route and recharge their batteries (e.g., Andelmin and Bartolini 2017; Baum et al. 2019; Erdoğan and Miller-Hooks 2012; Yi, Smart, and Shirk 2018). For instance, Baum et al. (2019) proposed a constrained shortest path problem (SPP) for BEVs that allows the vehicle to recharge its battery at charging stations along the route and ensures that the battery is not fully depleted during travel. They solved the problem using a charging function propagating algorithm, which is accelerated by heuristics. The second option is to plan routes that can be completed within the available battery capacity of the vehicle (e.g., Baum et al. 2020; Florio, Absi, and Feillet 2021; Pelletier, Jabali, and Laporte 2019; Yi and Bauer 2018). For example, Baum et al. (2020) investigated constrained SPPs for BEVs with the goal of reaching the destination as fast as possible while remaining within the vehicle's battery capacity. The vehicle can adjust its speed to balance the trade-off between energy consumption and travel time. They solved the problems using a trade-off function propagating algorithm, which is an exact algorithm, and made it more computationally efficient by integrating heuristics.

HEVs can operate in fuel, electric, boost, and charging modes, with the latter using fuel to recharge the battery. As a result, routing problems for HEVs should determine both the optimal routes and the appropriate running mode for each arc. Doppstadt, Koberstein, and Vigo (2016) considered an HEV TSP with each mode's cost and travel time on each road segment assumed to be known values. To solve the problem efficiently, they proposed a tabu search heuristic. In subsequent work, Doppstadt, Koberstein, and Vigo (2020) extended the problem by incorporating time windows for customers and proposed a variable neighborhood search heuristic. Additionally, Rocha and Subramanian (2023) proposed a hybrid genetic search for the HEV TSP with time windows, which outperforms the approach introduced by Doppstadt, Koberstein, and Vigo (2020) in terms of both computing time and solution quality. Liu, Miao, and Zhu (2019) first considered an SPP where the vehicle speed and route are jointly optimized, and used a hybrid powertrain control strategy to minimize the fuel consumption by distributing the power between different engines. The problem is an extension of the SPP and is solved by a genetic algorithm. De Nunzio, Gharbia, and Sciarretta (2021) calculated the energy consumption based on a predicted speed profile and investigated a general constrained eco-routing problem for HEVs to find an energy-minimal route. They evaluated several solution approaches for the problem and found the most effective method in terms of both accuracy and efficiency.

Compared to HEVs, PHEVs typically have larger batteries that can be charged from external electrical outlets and do not rely on fuel for charging. As a result, PHEVs can operate in fuel, electricity, and boost modes, and the routing problems also need to consider the operation mode for each arc. Various studies have investigated the routing problems of PHEVs. Sun and Zhou (2016) proposed an SPP that minimizes the traveling cost of a PHEV, and developed an algorithm based on dynamic programming to solve the problem optimally. Mancini (2017) introduced a PHEV vehicle routing problem (VRP) that minimizes the total travel distance and the penalty costs associated with using the fuel mode. The problem was solved by a large neighborhood search-based matheuristic. Nejad et al. (2017) proposed an energy-efficient SPP for PHEVs that minimizes fuel consumption. They proved that the problem is NP-complete and developed two exact algorithms based on dynamic programming and a fully polynomial time approximation scheme to solve the problem. In Bahrami et al. (2020), a PHEV's energy consumption is determined based on the driving cycle, resulting in a predetermined energy consumption on each road segment. The battery charge level is discretized into multiple levels, enabling the formulation of a four-index VRP, which is solved by a branch-and-price algorithm and a heuristic method.

Table 1 provides an overview of the reviewed literature. To the best of our knowledge, no existing work has integrated speed optimization and routing problems for PHEVs, particularly for the TSP. Such integration enables the vehicle to adjust its speed within the speed limit for a lower energy consumption cost. The integration of speed optimization and routing problems in freight transportation has been extensively studied in the literature (e.g., Baum et al. 2020; Dabia, Demir, and Woensel 2017; Demir, Bektaş, and Laporte 2012; Fukasawa et al. 2018; Macrina et al. 2019), and it has been demonstrated that incorporating speed optimization into routing problems can improve the energy efficiency of vehicles. Therefore, this paper aims to integrate speed optimization and TSP for a PHEV to explore the potential of reducing energy consumption.

Table 1: Comparison of the problem characteristics studied in this paper and in related papers

Papers	Vehicle	Problem	Charging stations	Speed optimization	Energy recuperation	Solution method
Bahrami et al. (2020)	PHEV	VRP	√	–	–	E & H
Baum et al. (2019)	BEV	SPP	√	–	√	E & H
Baum et al. (2020)	BEV	SPP	–	√	√	E & H
Caspari, Fahr, and Mitsos (2021)	HEV	SPP	–	–	√	E
De Nunzio, Gharbia, and Sciarretta (2021)	HEV	SPP	–	–	√	E
Doppstadt, Koberstein, and Vigo (2016)	HEV	TSP	–	–	–	H
Doppstadt, Koberstein, and Vigo (2020)	HEV	TSP	–	–	–	H
Florio, Absi, and Feillet (2021)	BEV	VRP	–	–	–	E
Liu, Miao, and Zhu (2019)	HEV	SPP	–	√	√	H
Pelletier, Jabali, and Laporte (2019)	BEV	VRP	–	–	–	E & H
Mancini (2017)	PHEV	VRP	√	–	–	H
Nejad et al. (2017)	PHEV	SPP	–	–	–	E & A
Sun and Zhou (2016)	PHEV	SPP	–	–	√	E
Rocha and Subramanian (2023)	HEV	TSP	–	–	–	H
Yi, Smart, and Shirk (2018)	BEV	SPP	√	–	√	E
Yi and Bauer (2018)	BEV	SPP	–	–	√	E
This paper	PHEV	TSP	√	√	√	E & H

[a] '–' means that the paper does not consider the feature, and '√' means that the paper considers the feature;
[b] In column 'Solution method', E, H, and A denote exact, heuristic, and approximation algorithms, respectively.

3 Problem definition

This section first presents an energy consumption model based on the vehicle speed (Section 3.1). Second, a mixed-integer nonlinear programming model for the PHEV-TSPS is described in Section 3.2.

Third, in Section 3.3, the nonlinear terms associated with vehicle speed in the PHEV-TSPS are linearized by discretizing speed. Finally, in Section 3.4, the proposed PHEV-TSPS model is extended to incorporate the presence of charging stations.

3.1 Energy consumption model

According to Barth, Younglove, and Scora (2005), Barth and Boriboonsomsin (2008), and Scora and Barth (2006), the total tractive power usage P_t (kilowatt/second) of the vehicle at time t can be calculated as follows:

$$P_t = (ma_t + mg\sin\theta_t + \frac{1}{2}C_d\rho Av_t^2 + C_r mg\cos\theta_t)v_t, \tag{1}$$

where a_t is the acceleration (meter/second^2), v_t is the speed (meter/second), m is the curb-weight (kilogram), θ_t is the road gradient (radian), g is the gravitational constant (meter/second^2), C_d is the coefficient of aerodynamic drag, C_r is the coefficient of rolling resistance, ρ is the air density (kilogram/meter^3), and A is the frontal surface area (meter^2). The typical values of the parameters are shown in Table 2.

Table 2: Description of the parameters in equation (1) and their typical values (Demir, Bektaş, and Laporte 2014)

Notation	Description	Typical value
m	Curb-weight (kilogram)	6350
g	Gravitational constant (meter/second^2)	9.81
C_d	Coefficient of aerodynamic drag	0.7
ρ	Air density (kilogram/meter^3)	1.2041
A	Frontal surface area (meter^2)	3.912
C_r	Coefficient of rolling resistance	0.01

Let T_S be the travel time of the road segment $[0, S]$, then the total tractive energy demand over a given road segment $[0, S]$ can be calculated as follows:

$$E_{tra} = \int_0^{T_S} P_t \mathrm{d}t. \tag{2}$$

Since the travel time depends on the vehicle speed, we reformulate the time-dependent function (2) as the following distance-dependent function via the transformation $\mathrm{d}t = \frac{\mathrm{d}s}{v}$ (see Hellström, Fröberg, and Nielsen 2006):

$$\begin{aligned} E_{tra} &= \int_0^S P_s \frac{\mathrm{d}s}{v_s} \\ &= \int_0^S Ma_s + mg\sin\theta_s + \frac{1}{2}C_d\rho Av_s^2 + C_r mg\cos\theta_s \ \mathrm{d}s. \end{aligned} \tag{3}$$

In Baum et al. (2020), Bektaş and Laporte (2011) and Demir, Bektaş, and Laporte (2014), the authors optimize the average speed on each road segment to reduce vehicle energy consumption under the assumption that the vehicle travels at a constant speed along the road segment and that the road gradient is constant. Their assumptions are not restrictive, because we can add intermediate nodes to mimic the changing conditions (Baum et al. 2020). Thus, we follow their assumptions and estimate the tractive-energy demand as follows:

$$E_{tra}(v) = \left(mg\sin\theta + \frac{1}{2}C_d\rho Av^2 + C_r mg\cos\theta\right)S, \tag{4}$$

where v and θ are the average speed and average road gradient, respectively. Function (4) shows that the energy consumption on a road segment has an approximate quadratic relationship with the average speed, which is consistent with vehicle energy consumption estimations in previous studies such as those of Baum et al. (2020) and Yi and Shirk (2018).

Without loss of generality, we ignore the engine power demand associated with running losses of the engine and additional vehicle accessories, which is often set as an exogenous parameter, such as 0 (Nasri, Bektaş, and Laporte 2018). When the vehicle is braking or driving downhill, $E_{tra}(v)$ could be negative, and PHEVs can sometimes recharge their batteries by using a motor generator. Let η_d and η_g be the drivetrain efficiency and regeneration efficiency, respectively. Then, the energy consumption can be calculated as the summation of the energy demand (positive) and the energy recuperation (negative) (Murakami 2017; Yi and Bauer 2018), as follows:

$$\begin{aligned} E(v) &= \frac{1}{\eta_d}\max\{E_{tra}(v),0\} + \eta_g \min\{E_{tra}(v),0\} \\ &= \left(\frac{1}{\eta_d} - \eta_g\right)\max\{E_{tra}(v),0\} + \eta_g \max\{E_{tra}(v),0\} + \eta_g \min\{E_{tra}(v),0\} \\ &= \left(\frac{1}{\eta_d} - \eta_g\right)\max\{E_{tra}(v),0\} + \eta_g E_{tra}(v). \end{aligned} \tag{5}$$

In practice, we usually have $0 < \eta_g < \eta_d < 1$ (Yi and Bauer 2018), thus $\frac{1}{\eta_d} - \eta_g$ is a positive value. When $\eta_g = 0$, function (5) calculates the energy consumption of a vehicle which is not equipped with an energy recuperation system.

3.2 The traveling salesman problem with speed optimization

The problem can be defined on a directed graph $G = (V, A)$, with a directed arc set A, a node set $V = \{0, 1, ..., n, n+1\}$, including the customers $i \in \{1, 2, ..., n\}$, the starting depot $0 \in V$ and the ending depot $n+1 \in V$, where the ending depot can coincide with the starting depot. The entire trip needs to be finished within a time budget T, which may be the driver's maximum working hours (Doppstadt, Koberstein, and Vigo 2016).

For each arc $(i, j) \in A$, let v_{ij} be the average travel speed, d_{ij} be the distance, and E_{ij} be the energy demand on arc (i, j) depending on the speed v_{ij}. We let $\mu \in [0, 1]$ be the coefficient of the electricity energy split in the boost mode, $V_i^+ = \{j | j \in V, (i, j) \in A\}$ be the set of tail nodes of the arcs whose head node is i, $V_i^- = \{j | j \in V, (j, i) \in A\}$ be the set of head nodes of the arcs whose tail node is i, $\underline{B}$ and $\overline{B}$ be the battery's minimum and maximum charge levels, respectively, and $\underline{v}_{ij}$ and $\overline{v}_{ij}$ be the lower and upper bounds on the speed, respectively. For each arc $(i, j) \in A$, let x_{ij} be a binary variable taking value 1 if and only if it is used in the route, x_{ij}^f be a binary variable taking value 1 if and only if the vehicle is running on the fuel mode, x_{ij}^e be a binary variable taking value 1 if and only if the vehicle is running on the electric mode, x_{ij}^r be a binary variable taking value 1 if and only if the vehicle is running on the energy recuperation mode, and x_{ij}^b be a binary variable taking value 1 if and only if the vehicle is running on the boost mode. For each node $i \in N$, let y_i and t_i be the state of charge and the arriving time at node i, respectively.

Our objective is to minimize the total cost of the energy consumption over the whole trip. Let the parameters c_f, c_e, c_b, and $-c_e$ be the unit cost of the energy consumption in fuel-only mode, electric-only mode, boost mode, and energy recuperation mode, respectively. Then the PHEV-TSPS can be formulated as follows:

$$\min \quad Z = \sum_{(i,j)\in A} \left(c_f x_{ij}^f + c_e x_{ij}^e + c_b x_{ij}^b\right) E_{ij} - c_e x_{ij}^r (y_j - y_i) \tag{6}$$

$$\begin{aligned} \text{s.t.} \quad E_{ij} = &\left(\frac{1}{\eta_d} - \eta_g\right) d_{ij} \max\left\{mg\sin\theta_{ij} + \frac{1}{2}C_d\rho A v_{ij}^2 + C_r mg\cos\theta_{ij}, 0\right\} \\ &+ \eta_g d_{ij}\left(mg\sin\theta_{ij} + \frac{1}{2}C_d\rho A v_{ij}^2 + C_r mg\cos\theta_{ij}\right) \qquad \forall (i,j) \in A \end{aligned} \tag{7}$$

$$x^f_{ij} + x^e_{ij} + x^b_{ij} + x^r_{ij} = x_{ij} \qquad \forall (i,j) \in A \tag{8}$$

$$\sum_{j \in V_i^+} x_{ij} = 1 \qquad \forall i \in V \backslash \{n+1\} \tag{9}$$

$$\sum_{i \in V_j^-} x_{ij} = 1 \qquad \forall j \in V \backslash \{0\} \tag{10}$$

$$\sum_{i \in \Omega} \sum_{j \notin \Omega} x_{ij} \geq 1 \qquad \forall \Omega \in V \backslash \{n+1\}, |\Omega| \geq 2 \tag{11}$$

$$(x^f_{ij} + x^e_{ij} + x^b_{ij} - 1) M_{ij} \leq E_{ij} \qquad \forall (i,j) \in A \tag{12}$$

$$(1 - x^r_{ij}) M_{ij} \geq E_{ij} \qquad \forall (i,j) \in A \tag{13}$$

$$\sum_{(i,j) \in A} x_{ij} \frac{d_{ij}}{v_{ij}} \leq T \tag{14}$$

$$y_i - \left(x^e_{ij} + \mu x^b_{ij} + x^r_{ij}\right) E_{ij} \geq y_j - (1 - x_{ij}) \overline{B} \qquad \forall (i,j) \in A \tag{15}$$

$$y_i - \left(x^e_{ij} + \mu x^b_{ij}\right) E_{ij} \leq y_j + (1 - x_{ij}) \overline{B} \qquad \forall (i,j) \in A \tag{16}$$

$$\underline{B} \leq y_i \leq \overline{B} \qquad \forall i \in V \backslash \{0\} \tag{17}$$

$$\underline{v}_{ij} \leq v_{ij} \leq \overline{v}_{ij} \qquad \forall (i,j) \in A \tag{18}$$

$$y_0 = \overline{B} \tag{19}$$

$$x_{ij}, x^f_{ij}, x^e_{ij}, x^b_{ij}, x^r_{ij} \in \{0, 1\} \qquad \forall (i,j) \in A, \tag{20}$$

where M_{ij} is a sufficiently large constant and can be set as the maximum absolute value of $E_{ij}, (i,j) \in A$, which can be calculated as the maximum value over the speed range.

The objective function (6) minimizes the total cost of the energy consumption over the whole trip, where the first term calculates the cost in fuel-only, electric-only, and boost modes, and the second term calculates the cost reduction by energy recuperation. Constraints (7) calculate the energy consumption (positive) or energy recuperation (negative) on arc (i,j). Constraints (8) ensure that the PHEV can only run in one mode on each arc. Constraints (9) and (10) ensure that every customer has one incoming and one outgoing arc. Constraints (11) are the subtour elimination constraints. Constraints (12) require that fuel-only, electric-only, and boost modes are not chosen under a negative energy consumption. Constraints (13) enforce that the energy recuperation mode cannot be chosen under a positive energy consumption. Constraint (14) requires that the journey is finished within the time budget. Constraints (15) and (16) determine the battery charging level at each node. Constraints (17) bound the battery charge level to a range between the minimum and maximum charge levels for the entire trip. Constraints (18) limit the speeds over the entire network. Here, we assume $\underline{v}_{ij} > 0$ to ensure constraints (14) are feasible. Constraint (19) sets the initial battery charge level as $\overline{B}$. Note that the battery's initial charge level y_0, depending on the user setting, can be any value between $\underline{B}$ and $\overline{B}$.

The value of joint optimization of speed, route, and operation modes

The PHEV-TSPS jointly optimizes route, speed, and operation modes. One natural question is whether the proposed joint optimization method is superior to the sequential optimization method, which first optimizes energy consumption, then optimizes operations modes. More precisely, we consider the following two-step solution procedure:

- *Step 1* optimizes the energy consumption over the whole journey, including speed optimization and route decision. The model is as follows:

$$\min \sum_{(i,j) \in A} x_{ij} E_{ij} \tag{21}$$

$$\text{s.t.} \quad x_{ij} \in \{0,1\} \qquad \forall (i,j) \in A \tag{22}$$
$$(7), (9)\text{–}(11), (14), (18),$$

where objective function (21) minimizes the energy consumption over the whole journey.

- *Step 2* minimizes the traveling cost by allocating the energy consumption on each arc to different operation modes. The model is as follows:

$$\min \quad \sum_{(i,j)\in A} \left(c_f x_{ij}^f + c_e x_{ij}^e + c_b x_{ij}^b\right) \hat{E}_{ij} - c_e x_{ij}^r (y_j - y_i) \tag{23}$$
$$\text{s.t.} \quad x_{ij}^f + x_{ij}^e + x_{ij}^b + x_{ij}^r = \hat{x}_{ij} \qquad \forall (i,j) \in A \tag{24}$$
$$x_{ij}^f, x_{ij}^e, x_{ij}^b, x_{ij}^r \in \{0,1\} \qquad \forall (i,j) \in A \tag{25}$$
$$(12)\text{–}(13), (15)\text{–}(17), (19),$$

where $\hat{x}_{ij}, \hat{E}_{ij}$ are the optimized route and energy consumption calculated in *Step 1*, respectively (the symbol $\hat{}$ is used to represent the known values).

The following proposition is introduced to show the difference between the sequential optimization method above and the PHEV-TSPS, and the proof is provided in Appendix B.

Proposition 1. *A solution from the sequential optimization approach following Steps 1 and 2 above has an energy consumption cost greater than or equal to that of the PHEV-TSPS.*

3.3 PHEV-TSPS with speed discretization

In order to reduce the computational complexity introduced by the nonlinear terms associated with variables v_{ij} in PHEV-TSPS, we can discretize the continuous speed into a discrete set of speed levels. Following the approach presented by Bektaş and Laporte (2011), let $\underline{v}_{\min} = \min\{\underline{v}_{ij}, (i,j) \in A\}$ and $\overline{v}_{\max} = \max\{\overline{v}_{ij}, (i,j) \in A\}$. We first discretize the speed range $[\underline{v}_{\min}, \overline{v}_{\max}]$ into a set of speed levels $L = \{0, 1, ..., l, ...\}$, where each level $l \in L$ corresponds to a speed level ν_l and $\nu_0 = \underline{v}_{\min}$, $\nu_{|L|} = \overline{v}_{\max}$. We then introduce a new binary variable z_{ijl} taking value 1 if the vehicle travels at the speed level ν_l on arc (i,j), and 0 otherwise. The variables z_{ijl} and x_{ij} are linked by the following equations:

$$\sum_{l\in L} z_{ijl} = x_{ij} \qquad \forall (i,j) \in A \tag{26}$$
$$z_{ijl} \in \{0,1\} \qquad \forall (i,j) \in A, l \in L. \tag{27}$$

Note that the speed ranges on different arcs can be different, the biggest range $[\underline{v}_{\min}, \overline{v}_{\max}]$ is used here only for the sake of simplicity in notation. By using the speed discretization, constraints (7) and (14) are reformulated as follows:

$$\begin{aligned} E_{ij} = {} & \left(\frac{1}{\eta_d} - \eta_g\right) d_{ij} \max\left\{ mg\sin\theta_{ij} + \frac{1}{2} C_d \rho A \sum_{l\in L} z_{ijl}\nu_l^2 + C_r mg \cos\theta_{ij}, 0 \right\} \\ & + \eta_g d_{ij} \left(mg\sin\theta_{ij} + \frac{1}{2} C_d \rho A \sum_{l\in L} z_{ijl}\nu_l^2 + C_r mg\cos\theta_{ij} \right) \qquad \forall (i,j) \in A \end{aligned} \tag{28}$$

$$\sum_{(i,j)\in A, l\in L} z_{ijl} \frac{d_{ij}}{\nu_l} \le T. \tag{29}$$

Finally, the PHEV-TSPS is converted to (6), (8)–(13), (15)–(20), (26)–(29), which we refer to as PHEV-TSPSD.

In the PHEV-TSPSD formulation, the vehicle can only drive at one speed out of the given discretized speed levels, so the feasible speed range is smaller than in the PHEV-TSPS, where the speed range is continuous. Therefore, the PHEV-TSPSD has an energy consumption cost that is higher than or equal to that of the PHEV-TSPS. Increasing the number of discretized speed levels can reduce the gap between the PHEV-TSPSD and the PHEV-TSPS, but can increase the computational complexity of the PHEV-TSPSD due to the presence of more integer variables, which will be tested later in the computational experiments.

3.4 PHEV-TSPS with charging stations at customer locations

Following the setting in Bahrami et al. (2020), we assume that the charging stations are located at specific customer locations, which are denoted by the set V^c. Here we assume a constant charging rate ϵ at each charging station, such that the recharging time is directly proportional to the amount of energy that needs to be recharged (Desaulniers et al. 2016; Keskin and Çatay 2018). In addition, the PHEV is allowed to be partially recharged, which means that the charging time τ_i at customer i is a decision variable. To simplify the notation, we set the recharging time at nodes without charging stations to be zero, namely $\tau_i = 0, \forall i \in V \backslash V^c$. The problem can then be formulated as follows:

$$\min \quad Z = \sum_{(i,j)\in A} \left(c_f x_{ij}^f + c_e x_{ij}^e + c_b x_{ij}^b \right) E_{ij} - c_e x_{ij}^r (y_j - y_i - \epsilon \tau_i) \tag{30}$$

$$\text{s.t.} \quad \sum_{(i,j)\in A} x_{ij} \frac{d_{ij}}{v_{ij}} + \sum_{i\in V} \tau_i \leq T \tag{31}$$

$$y_i - \left(x_{ij}^e + \mu x_{ij}^b + x_{ij}^r \right) E_{ij} + \epsilon \tau_i \geq y_j - (1 - x_{ij}) \overline{B} \qquad \forall (i,j) \in A \tag{32}$$

$$y_i - \left(x_{ij}^e + \mu x_{ij}^b \right) E_{ij} + \epsilon \tau_i \leq y_j + (1 - x_{ij}) \overline{B} \qquad \forall (i,j) \in A \tag{33}$$

$$\tau_i = 0 \qquad \forall i \in V \backslash V^c \tag{34}$$

(7)–(13), (17)–(20).

The second term in the left-hand side of constraint (31) calculates the total recharging time. The third term of the left-hand side of constraints (32)–(33) represents the amount of energy recharged at each customer location. We will use the name PHEV-TSPS-CS to refer to the model above. In addition, we have included a model in Appendix A to show that our approach can also be applied to scenarios with charging stations that are not solely located at customer premises.

4 Valid inequalities

To reduce the computation time for solving the models presented in the previous section, this section introduces new valid inequalities to strengthen the models.

4.1 Energy accumulation inequality

Let the optimal tour of the PHEV-TSPS be A_p, where $x_{ij} = 1, \forall (i,j) \in A_p$, then we can obtain the following constraint by aggregating constraints (15) over the optimal tour:

$$\begin{aligned}
&\sum_{(i,j)\in A_p} (x_{ij}^e + \mu x_{ij}^b + x_{ij}^r) E_{ij} \leq \sum_{(i,j)\in A_p} (y_i - y_j) + (1 - x_{ij}) \bar{B} \\
\iff &\sum_{(i,j)\in A_p} (x_{ij}^e + \mu x_{ij}^b + x_{ij}^r) E_{ij} \leq y_0 - y_{n+1} \\
\iff &\sum_{(i,j)\in A_p} (x_{ij}^e + \mu x_{ij}^b + x_{ij}^r) E_{ij} + \sum_{(i,j)\in A\backslash A_p} (x_{ij}^e + \mu x_{ij}^b + x_{ij}^r) E_{ij} \leq y_0 - y_{n+1} \\
\iff &\sum_{(i,j)\in A} x_{ij}^e E_{ij} + \mu \sum_{(i,j)\in A} x_{ij}^b E_{ij} + \sum_{(i,j)\in A} x_{ij}^r E_{ij} \leq y_0 - y_{n+1},
\end{aligned} \tag{35}$$

where the first equality is derived from the fact that $x_{ij} = 1, \forall (i,j) \in A_p$ and the second equality is based on the fact that $x^e_{ij} = 0, x^b_{ij} = 0, x^r_{ij} = 0, \forall (i,j) \in A \backslash A_p$.

We refer to this new inequality as the 'energy accumulation inequality', which can be easily integrated into the model as a standard constraint. Although it appears simple, it has a significant potential to accelerate computations, as demonstrated in the computational experiments.

We can also derive the following inequality based on constraints (32) for PHEV-TSPS-CS:

$$\sum_{(i,j)\in A} x^e_{ij} E_{ij} + \mu \sum_{(i,j)\in A} x^b_{ij} E_{ij} + \sum_{(i,j)\in A} x^r_{ij} E_{ij} \leq y_0 - y_{n+1} + \epsilon \sum_{i\in V} \tau_i. \tag{36}$$

4.2 Lower bound inequalities

Before introducing the lower bound for PHEV-TSPS, we first introduce the following lemma, whose proof is given in Appendix B:

Lemma 1. *Objective function (6) is equal to the following expression:*

$$\min \quad Z = \sum_{(i,j)\in A} \left(c_f x^f_{ij} + c_e x^e_{ij} + c_b x^b_{ij} + c_e x^r_{ij} \right) E_{ij}. \tag{37}$$

By relaxing terms $\sum_{(i,j)\in A} x^f_{ij} E_{ij}$, $\sum_{(i,j)\in A} x^e_{ij} E_{ij}$, and $\sum_{(i,j)\in A} x^b_{ij} E_{ij}$ to three continuous variables Z_f, Z_e, and Z_b, respectively, we can obtain an objective function which is a lower bound of the objective function (37). This lower bound represents allocating the energy consumption (except the energy recuperation) over the whole journey to different operation modes:

$$\min \quad c_f Z_f + c_e Z_e + c_b Z_b + c_e \sum_{(i,j)\in A} x^r_{ij} E_{ij} \tag{38}$$

$$\text{s.t.} \quad Z_f + Z_e + Z_b = \sum_{(i,j)\in A} \left(x_{ij} E_{ij} - x^r_{ij} E_{ij} \right) \tag{39}$$

$$Z_e + \mu Z_b \leq y_0 - y_{n+1} - \sum_{(i,j)\in A} x^r_{ij} E_{ij} \tag{40}$$

$$Z_f \geq 0, Z_e \geq 0, Z_b \geq 0, \tag{41}$$

where the first constraint is due to constraints (8), and the second constraint is a result of the energy accumulation inequality.

Model (38)–(41) above can be deemed as a linear programming model with decision variables Z_f, Z_e, and Z_b, and can be solved analytically. Following this approach, Propositions 2 and 3 are developed to calculate a lower bound for PHEV-TSPS and PHEV-TSPSD, and their proofs are provided in Appendix B. Due to the fact that electricity is cheaper than fuel, here we assume $c_e \leq c_b \leq c_f$.

Proposition 2. *If $\frac{c_f - c_b}{\mu} \leq c_f - c_e$, we introduce two new continuous variables κ_1, κ_2 and two new binary variables δ_1, δ_2, then the following inequalities are valid for the PHEV-TSPS:*

$$Z \geq c_e \kappa_1 + \frac{(y_0 - y_{n+1} - \sum_{(i,j)\in A} x^r_{ij} E_{ij})(c_e - c_b)}{1-\mu} \delta_2 + \frac{c_b - \mu c_e}{1-\mu} \kappa_2 + c_e \sum_{(i,j)\in A} x^r_{ij} E_{ij} \tag{42}$$

$$\kappa_1 + \kappa_2 = \sum_{(i,j)\in A} \left(x_{ij} E_{ij} - x^r_{ij} E_{ij} \right) \tag{43}$$

$$\kappa_1 \leq (y_0 - y_{n+1} - \sum_{(i,j)\in A} x^r_{ij} E_{ij}) \delta_1 \tag{44}$$

$$(y_0 - y_{n+1} - \sum_{(i,j)\in A} x^r_{ij} E_{ij}) \delta_2 \leq \kappa_2 \leq M \delta_2 \tag{45}$$

$$\delta_1 + \delta_2 = 1 \tag{46}$$

$$\delta_1, \delta_2 \in \{0, 1\}, \tag{47}$$

where M is a sufficiently large constant and can be set as $\sum_{(i,j)\in A} M_{ij}$.

Proposition 3. *If $\frac{c_f - c_b}{\mu} > c_f - c_e$, we introduce three new continuous variables $\kappa_1, \kappa_2, \kappa_3$ and three new binary variables $\delta_1, \delta_2, \delta_3$, the following inequalities are valid for the PHEV-TSPS:*

$$Z \geq c_e\kappa_1 + \frac{(y_0 - y_{n+1} - \sum_{(i,j)\in A} x^r_{ij}E_{ij})(c_e - c_b)}{1-\mu}\delta_2 + \frac{c_b - \mu c_e}{1-\mu}\kappa_2 + \frac{(y_0 - y_{n+1} - \sum_{(i,j)\in A} x^r_{ij}E_{ij})(c_b - c_f)}{1-\mu}\delta_3 + c_f\kappa_3 + c_e \sum_{(i,j)\in A} x^r_{ij}E_{ij} \tag{48}$$

$$\kappa_1 + \kappa_2 + \kappa_3 = \sum_{(i,j)\in A} \left(x_{ij}E_{ij} - x^r_{ij}E_{ij}\right) \tag{49}$$

$$\kappa_1 \leq (y_0 - y_{n+1} - \sum_{(i,j)\in A} x^r_{ij}E_{ij})\delta_1 \tag{50}$$

$$(y_0 - y_{n+1} - \sum_{(i,j)\in A} x^r_{ij}E_{ij})\delta_2 \leq \kappa_2 \leq \frac{(y_0 - y_{n+1} - \sum_{(i,j)\in A} x^r_{ij}E_{ij})\delta_2}{\mu} \tag{51}$$

$$\frac{(y_0 - y_{n+1} - \sum_{(i,j)\in A} x^r_{ij}E_{ij})\delta_3}{\mu} \leq \kappa_3 \leq M\delta_3 \tag{52}$$

$$\delta_1 + \delta_2 + \delta_3 = 1 \tag{53}$$

$$\delta_1, \delta_2, \delta_2 \in \{0, 1\}. \tag{54}$$

Since the number of valid inequalities in Propositions 2 and 3 is quite small, they can be directly added as standard constraints to the PHEV-TSPS and the PHEV-TSPSD. For the PHEV-TSPS-CS, the inequalities proposed in Propositions 2 and 3 can be made valid by substituting the term $y_0 - y_{n+1}$ with the term $y_0 - y_{n+1} + \epsilon \sum_{i\in V} \tau_i$.

5 Solution method

In this section, we introduce the method to solve the proposed PHEV-TSPS. Section 5.1 introduces the subgradient cut for the PHEV-TSPS to eliminate the nonlinear terms associated with vehicle speed. Section 5.2 linearizes the proposed PHEV-TSPS to a mixed-integer linear programming (MILP) model. Section 5.3 develops a branch-and-cut algorithm based on the MILP model. Note that the methods proposed in this section can be applied to the PHEV-TSPSD, with the exception of the subgradient cut. In addition, all of the methods can be applied to the PHEV-TSPS-CS with slight modifications, the details of which can be found in Appendix C.

5.1 Subgradient cut

The nonlinear terms v^2_{ij} and $\frac{1}{v_{ij}}$ in the PHEV-TSPS make the problem intractable. To eliminate the nonlinear terms, we first introduce new variables $u_{ij} = v^2_{ij}, (i,j) \in A$. Then, constraints (7), (14), and (18) can be reformulated as follows:

$$E_{ij} = \left(\frac{1}{\eta_d} - \eta_g\right) d_{ij} \max\left\{mg\sin\theta_{ij} + \frac{1}{2}C_d\rho A u_{ij} + C_r mg\cos\theta_{ij}, 0\right\} + \eta_g d_{ij}\left(mg\sin\theta_{ij} + \frac{1}{2}C_d\rho A u_{ij} + C_r mg\cos\theta_{ij}\right) \quad \forall (i,j) \in A \tag{55}$$

$$\sum_{(i,j)\in A} d_{ij}x_{ij}u_{ij}^{-\frac{1}{2}} \leq T \tag{56}$$

$$\underline{v}_{ij}^2 \leq u_{ij} \leq \overline{v}_{ij}^2 \qquad \forall (i,j) \in A. \tag{57}$$

Because of the minimization in the objective function, equations (55) can be linearized into the following constraints:

$$E_{ij} \geq \frac{d_{ij}}{\eta_d}\left(mg\sin\theta_{ij} + \frac{1}{2}C_d\rho A u_{ij} + C_r mg\cos\theta_{ij}\right) + (x_{ij}-1)M_{ij} \qquad \forall (i,j) \in A \tag{58}$$

$$E_{ij} \geq \eta_g d_{ij}\left(mg\sin\theta_{ij} + \frac{1}{2}C_d\rho A u_{ij} + C_r mg\cos\theta_{ij}\right) + (x_{ij}-1)M_{ij} \qquad \forall (i,j) \in A. \tag{59}$$

Constraints (56) are nonlinear because of the term $u_{ij}^{-\frac{1}{2}}$, which is a convex function in u_{ij}. Similarly to the approach of Cheng, Adulyasak, and Rousseau (2020), we can derive a subgradient cut as follows:

- **First**, by substituting term $u_{ij}^{-\frac{1}{2}}$ with a new continuous variable q_{ij}, constraint (56) are reformulated to the following constraint:

$$\sum_{(i,j)\in A} d_{ij}x_{ij}q_{ij} \leq T. \tag{60}$$

  Constraint (60) is nonlinear because of term $x_{ij}q_{ij}$, and can be converted to the following linear constraint:

$$\sum_{(i,j)\in A} d_{ij}q_{ij} \leq T \tag{61}$$

$$q_{ij} \geq 0 \qquad \forall (i,j) \in A. \tag{62}$$

- **Second**, the tangent line of function $u_{ij}^{-\frac{1}{2}}$ at point $(\hat{u}_{ij}, \hat{u}_{ij}^{-\frac{1}{2}})$ is $-\frac{1}{2}\hat{u}_{ij}^{-\frac{3}{2}}(u_{ij} - \hat{u}_{ij}) + \hat{u}_{ij}^{-\frac{1}{2}}$, as shown in Figure 1. Then the subgradient cut for term $u_{ij}^{-\frac{1}{2}}$ can be derived as follows:

$$q_{ij} \geq -\frac{1}{2}\hat{u}_{ij}^{-\frac{3}{2}}(u_{ij} - \hat{u}_{ij}x_{ij}) + \hat{u}_{ij}^{-\frac{1}{2}}x_{ij} \qquad \forall (i,j) \in A. \tag{63}$$

  If $x_{ij} = 0$, the right-hand side of constraints (63) will be negative and the cut is inactive; else, the cut is added to the problem.

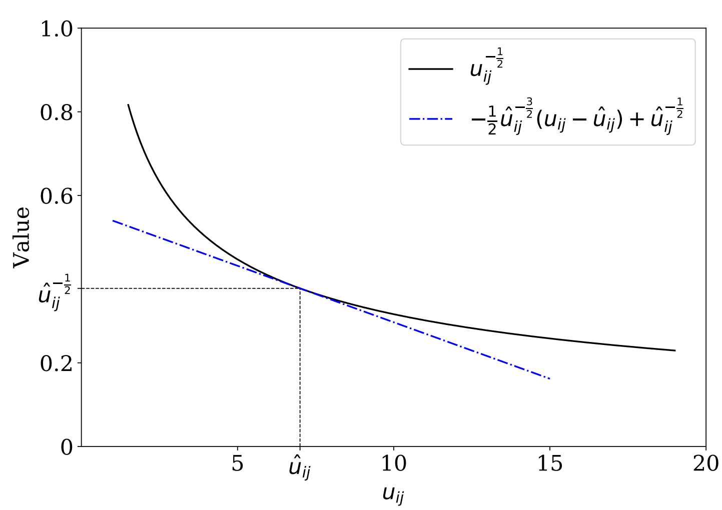

Figure 1: The tangent line of function $u_{ij}^{-\frac{1}{2}}$ at point $(\hat{u}_{ij}, \hat{u}_{ij}^{-\frac{1}{2}})$

5.2 Linearization

In this section, we first linearize the PHEV-TSPS into an MILP model, and then linearize the valid inequalities proposed in Section 4.

5.2.1 PHEV-TSPS

The products of binary variables and continuous variables $x^f_{ij}E_{ij}$, $x^b_{ij}E_{ij}$, $x^e_{ij}E_{ij}$, and $x^r_{ij}E_{ij}$ can be replaced by new continuous variables w^f_{ij}, w^b_{ij}, w^e_{ij}, and w^r_{ij} with the following constraints:

$$w^f_{ij} + w^b_{ij} + w^e_{ij} + w^r_{ij} \geq E_{ij} \qquad \forall (i,j) \in A \tag{64}$$
$$w^f_{ij} \leq x^f_{ij} M_{ij} \qquad \forall (i,j) \in A \tag{65}$$
$$w^b_{ij} \leq x^b_{ij} M_{ij} \qquad \forall (i,j) \in A \tag{66}$$
$$w^e_{ij} \leq x^e_{ij} M_{ij} \qquad \forall (i,j) \in A \tag{67}$$
$$-x^r_{ij} M_{ij} \leq w^r_{ij} \qquad \forall (i,j) \in A \tag{68}$$
$$w^f_{ij}, w^b_{ij}, w^e_{ij} \geq 0, w^r_{ij} \leq 0 \qquad \forall (i,j) \in A. \tag{69}$$

Now, objective function (37) can be rewritten as follows:

$$\min \quad Z = \sum_{(i,j)\in A} c_f w^f_{ij} + c_e w^e_{ij} + c_b w^b_{ij} + c_e w^r_{ij} \tag{70}$$
$$\text{s.t.} \quad (64)\text{–}(69).$$

By using the new variables defined above, constraints (15)–(16) can be reformulated as the following linear constraints:

$$y_i - w^e_{ij} - \mu w^b_{ij} - w^r_{ij} \geq y_j - (1 - x_{ij})\overline{B} \qquad \forall (i,j) \in A \tag{71}$$
$$y_i - w^e_{ij} - \mu w^b_{ij} \leq y_j + (1 - x_{ij})\overline{B} \qquad \forall (i,j) \in A. \tag{72}$$

Finally, the PHEV-TSPS is reformulated into (8)–(13), (17), (19)–(20), (57)–(59), (61)–(72), which is an MILP model.

5.2.2 Valid inequalities

Applying the variables defined in the last subsection, energy accumulation inequality (35) can be converted to the following inequality:

$$\sum_{(i,j)\in A} w^e_{ij} + \mu w^b_{ij} + w^r_{ij} \leq y_0 - y_{n+1}. \tag{73}$$

Using the fact that energy consumption beyond the chosen route does not contribute to the total energy consumption cost, we modify constraints (18) and (58)–(59) as follows:

$$x_{ij}\underline{v}^2_{ij} \leq u_{ij} \leq x_{ij}\overline{v}^2_{ij} \qquad \forall (i,j) \in A \tag{74}$$
$$E_{ij} \geq \frac{d_{ij}}{\eta_d}\left(x_{ij} mg \sin\theta_{ij} + \frac{1}{2} C_d \rho A u_{ij} + x_{ij} C_r mg \cos\theta_{ij} \right) \qquad \forall (i,j) \in A \tag{75}$$
$$E_{ij} \geq \eta_g d_{ij}\left(x_{ij} mg \sin\theta_{ij} + \frac{1}{2} C_d \rho A u_{ij} + x_{ij} C_r mg \cos\theta_{ij} \right) \qquad \forall (i,j) \in A. \tag{76}$$

Now, the term E_{ij} for arcs outside the selected tour is equal to 0. Thus, the term $x_{ij}E_{ij}$ in the valid inequalities can be replaced with E_{ij}.

For valid inequalities (42)–(45), we introduce a new variable σ_1 subject to the following constraints:

$$\sigma_1 \leq y_0 - y_{n+1} - \sum_{(i,j)\in A} w^r_{ij} + (1-\delta_2)M^* \tag{77}$$

$$\sigma_1 \leq \delta_2 M^*, \tag{78}$$

where M^* is the upper bound of $y_0 - y_{n+1} - \sum_{(i,j)\in A} w^r_{ij}$. Then, the inequalities can be linearized as follows:

$$Z \geq c_e\kappa_1 + \frac{(c_e - c_b)}{1-\mu}\sigma_1 + \frac{c_b - \mu c_e}{1-\mu}\kappa_2 + c_e \sum_{(i,j)\in A} w^r_{ij} \tag{79}$$

$$\kappa_1 + \kappa_2 = \sum_{(i,j)\in A} \left(E_{ij} - w^r_{ij}\right) \tag{80}$$

$$\kappa_1 \leq \delta_1 M^* \tag{81}$$

$$\kappa_1 \leq y_0 - y_{n+1} - \sum_{(i,j)\in A} w^r_{ij} + (1-\delta_1)M^* \tag{82}$$

$$-\delta_2 M^* \leq \kappa_2 \leq \delta_2 M^* \tag{83}$$

$$\kappa_2 \geq y_0 - y_{n+1} - \sum_{(i,j)\in A} w^r_{ij} - (1-\delta_2)M^*. \tag{84}$$

For valid inequalities (48)–(49), we introduce a new variable σ_2 subject to the following constraints:

$$\sigma_2 \leq y_0 - y_{n+1} - \sum_{(i,j)\in A} w^r_{ij} + (1-\delta_3)M^* \tag{85}$$

$$\sigma_2 \leq \delta_3 M^*. \tag{86}$$

Then, the inequalities can be linearized as follows:

$$Z \geq c_e\kappa_1 + \frac{c_e - c_b}{1-\mu}\sigma_1 + \frac{c_b - \mu c_e}{1-\mu}\kappa_2 + \frac{c_b - c_f}{1-\mu}\sigma_2 + c_f\kappa_3 + c_e \sum_{(i,j)\in A} w^r_{ij} \tag{87}$$

$$\kappa_1 + \kappa_2 + \kappa_3 = \sum_{(i,j)\in A} \left(E_{ij} - w^r_{ij}\right) \tag{88}$$

$$\kappa_1 \leq \delta_1 M^* \tag{89}$$

$$\kappa_1 \leq y_0 - y_{n+1} - \sum_{(i,j)\in A} w^r_{ij} + (1-\delta_1)M^* \tag{90}$$

$$-\delta_2 M^* \leq \kappa_2 \leq \delta_2 M^* \tag{91}$$

$$y_0 - y_{n+1} - \sum_{(i,j)\in A} w^r_{ij} - (1-\delta_2)M^* \leq \kappa_2 \leq \frac{(y_0 - y_{n+1} - \sum_{(i,j)\in A} w^r_{ij} + (1-\delta_2) * M^*)}{\mu} \tag{92}$$

$$-\delta_3 M^* \leq \kappa_3 \leq \delta_3 M^* \tag{93}$$

$$\mu\kappa_3 \geq y_0 - y_{n+1} - \sum_{(i,j)\in A} w^r_{ij} - (1-\delta_3)M^*. \tag{94}$$

5.3 Branch-and-cut algorithm

Branch-and-cut is an exact solution procedure that has been effectively applied to solve different variants of the TSP (e.g., Alba Martínez et al. 2013; Cordeau, Ghiani, and Guerriero 2014). This section describes some of the key aspects of the algorithm that we have implemented to solve the proposed model.

Initialization: Since the energy recuperation mode cannot be selected when there is positive energy consumption, we calculate $\underline{E}_{ij}$ with the lower speed limit $\underline{v}_{ij}$ on each arc and set $x^r_{ij} = 0$ if $\underline{E}_{ij} > 0$.

Separation problem: For the subtour elimination constraints (11), we use a separation routine based on the minimum s-t cut algorithm proposed by Stoer and Wagner (1997). If a solution at a branch-and-bound node violates the subtour elimination constraints, the violated constraints are added to the model and the problem at the current node is resolved. This process is repeated until no violated constraints remain.

Subgradient cut: When an integer solution satisfying the subtour elimination constraints is found, subgradient cuts (63) can be derived from the current solution and added to the model. The problem is then solved again, and this process is repeated until no more subgradient cuts can be generated.

Battery flow constraints: During computational experiments, it was observed that the branch-and-cut algorithm can be accelerated by temporarily removing constraints (71)–(72) from the model, and only adding them back when an integer solution satisfying the subtour elimination constraints is found.

Branching priority: In our preliminary test, we observed that extremely long arcs caused issues for the branch-and-cut algorithm, resulting in increased computation times. To address this issue, we employed the k-means clustering technique (Pedregosa et al. 2011) to partition arcs into different clusters based on their length. Subsequently, we increased the branching priorities for the clusters containing longer arcs.

6 Numerical studies

This section presents the computational experiments undertaken to investigate the performance of the models and solution methods proposed in this paper. Section 6.1 introduces the instances used for the numerical testing. Section 6.2 assesses the performance of the proposed solution method. This is followed by a comparison with the solution method of Doppstadt, Koberstein, and Vigo (2016) in Section 6.3. Section 6.4 investigates the value of joint optimization of speed, route, and operation modes. Section 6.5 evaluates the impacts of road gradient and energy recuperation on the energy consumption cost. Section 6.6 investigates the impact of the presence of charging stations on the proposed model. All experiments are performed on an AMD Rome 7532 2.40 GHz 256M cache L3 CPU, the optimization models are solved using the Gurobi Optimizer 9.5.2, and the computing time limit is set to 7200 seconds. The instances and codes are available at the following URL: `https://github.com/fuliang93/PHEV-TSPS.git`.

6.1 Instances

This section evaluates the proposed methods using the instances of Doppstadt, Koberstein, and Vigo (2016), which consist of 36 instances that can be obtained from Doppstadt, Koberstein, and Vigo (2019). The instances are divided into three groups based on the distances between the depot and the delivery area (0, 28, and 57 kilometers). Each group contains instances with different numbers of customers: 8, 10, 20, and 50. To provide a more thorough investigation of the proposed methods, we also selected 30 or 40 customers from the original instances that contained 50 customers, resulting in instances with 30 or 40 customers, respectively. Additionally, we randomly generated 10 and 20 additional customers to create instances with 60 and 70 customers, respectively. The instances are denoted by HEVTSP_α_β_π, where α, β, and π represent the distances between the depot and the delivery area (1, 2, and 3 correspond to 0, 28, and 57 kilometers, respectively), the number of customers, and various customer locations.

The time budgets for $\alpha = 1, 2, 3$ are set to be 3600, 7200, and 10800 seconds, respectively. For each arc, we randomly select the speed limit $\overline{v}_{ij}$ from 15 to 19 meters/second and set the lower speed limit

$\underline{v}_{ij}$ to 3 meters/second. The upper battery limit $\overline{B}$ is set to 14.4 kilowatt-hours (the battery size of a 2022 Ford Escape PHEV (Latham 2022)), and the lower battery limit $\underline{B}$ is set to 0 kilowatt-hours. The unit costs for different modes c_f, c_e, c_b are set to 1.0, 0.5, and 0.7, respectively. For each instance, we randomly generate the elevation of each node, ranging from 0 to 100 meters, which is then utilized to calculate the slopes of the road between the nodes.

6.2 Performance of the solution method

This section describes the numerical experiments performed using the PHEV-TSPS model proposed in Section 3.2, along with the valid inequalities introduced in Section 4 and the solution methods discussed in Section 5.

First, we evaluate the effectiveness of the proposed valid inequalities. The computational results are summarized in Table 3, and the details can be found in Table 8 in Appendix D. We solve the PHEV-TSPS without valid inequalities using Gurobi, and we can observe that for most instances with 20 or 30 customers, optimality is not achieved within 2 hours. However, the computation efficiency is significantly improved with the energy accumulation inequality or the lower bound. All instances with 20 customers are solved to optimality within 1 minute, and most instances with 30 customers are solved to optimality within 2 hours. Moreover, the combination of the energy accumulation inequality and lower bound enables solving all instances with 30 customers to optimality within 1 hour, and the calculation time can be further reduced to less than 15 minutes by incorporating the branching priority. For the sake of clarity and consistency, we will refer to the PHEV-TSPS with all valid inequalities and branching priority as PHEV-TSPS-VI, and the PHEV-TSPSD with all valid inequalities and branching priority as PHEV-TSPSD-VI in the following experiments.

Table 3: Performances of the solution methods for PHEV-TSPS

		Original			*LB*			*EAI*			*LB + EAI*			*LB + EAI + BP*		
#Cus	*#Ins*	*#Opt*	*aTime*	*aGap*	*#Opt*	*aTime*	*aGap*	*#Opt*	*aTime*	*aGap*	*#Opt*	*aTime*	*aGap*	*#Opt*	*aTime*	*aGap*
8	9	9	8	0.0	9	1	0.0	9	1	0.0	9	1	0.0	9	1	0.0
10	9	9	203	0.0	9	3	0.0	9	2	0.0	9	2	0.0	9	2	0.0
20	9	3	4820	14.5	9	38	0.0	9	27	0.0	9	25	0.0	9	29	0.0
30	9	1	6406	19.7	8	2642	0.1	9	664	0.0	9	377	0.0	9	216	0.0
Total	36	22	2859	8.5	35	671	0.0	36	174	0.0	36	101	0.0	36	62	0.0

[a] *Original*: original PHEV-TSPS without valid inequalities; *LB*: PHEV-TSPS with the lower bound; *EAI*: PHEV-TSPS with the energy accumulation inequality; *LB + EAI*: PHEV-TSPS with the *LB* and *EAI*; *LB + EAI + BP*: PHEV-TSPS with the *LB*, *EAI*, and branching priority;
[b] *#Cus*: the number of customers; *#Ins*: the number of instances; *#Opt*: the number of instances that are solved to optimality within 2 hours; *aTime*: the average computation time (s); *aGap*: average optimality gap (%).

Second, we evaluate the performance of PHEV-TSPS-VI and PHEV-TSPSD-VI under instances with a higher number of customers, and the computation results are summarized in Table 4, with details in Tables 9–10 in Appendix D. All instances with 50 customers are solved to optimality using PHEV-TSPS-VI and PHEV-TSPSD-VI. However, for instances with more than 50 customers, most of them cannot be solved to optimality with PHEV-TSPS-VI. On the other hand, most of them can be solved to optimality with PHEV-TSPSD-VI by setting the speed discretization level to either 0.3 or 0.5 meter/second. For all instances, although the objective values obtained by PHEV-TSPSD-VI are slightly higher than those obtained by PHEV-TSPS-VI, the difference is negligible. Hence, PHEV-TSPSD-VI can be considered a viable option for cases that do not require exact solutions, and its computational efficiency can be further improved by increasing the speed discretization value.

Table 4: Performances of PHEV-TSPS-VI and PHEV-TSPSD-VI

		PHEV-TSPS-VI		Speed Discretization								
				0.1 (m/s)			0.3 (m/s)			0.5 (m/s)		
$\#Cus$	$\#Ins$	$\#Opt$	$aTime$	$\#Opt$	$aTime$	$Diff$	$\#Opt$	$aTime$	$Diff$	$\#Opt$	$aTime$	$Diff$
8	9	9	1	9	2	0.04	9	1	0.09	9	1	0.11
10	9	9	2	9	4	0.01	9	1	0.05	9	1	0.06
20	9	9	29	9	72	0.01	9	38	0.06	9	22	0.11
30	9	9	216	9	229	0.02	9	98	0.08	9	67	0.13
40	9	9	934	9	1097	0.02	9	351	0.08	9	539	0.15
50	9	9	3065	9	2491	0.02	9	714	0.06	9	514	0.10
60	9	2	6101	7	4968	_	8	2560	_	9	927	_
70	9	0	7200	0	7200	_	6	4395	_	8	3328	_
Total	72	56	2193	61	2008	_	68	1020	_	71	675	_

[a] $Diff$: the percentage increase (positive) or decrease (negative) compared to PHEV-TSPS-VI.

6.3 Comparison to Doppstadt, Koberstein, and Vigo (2016)

In this section, we compare our proposed solution method with the heuristic proposed by Doppstadt, Koberstein, and Vigo (2016). The TSP for HEV proposed by Doppstadt, Koberstein, and Vigo (2016) is based on an HEV with four operation modes, namely pure combustion, pure electric, charging, and boost modes. A key difference between their HEV and our PHEV is that their battery can only be charged using fuel and not by a charging station. However, their charging mode is similar to our energy recuperation mode, where the battery can be charged during travel. Consequently, their model has a structure that is similar to the PHEV-TSPS with fixed speeds, where the cost and travel time on each arc are fixed.

To compare with their method, we first modify our proposed PHEV-TSPS to their case. Here, we use the binary variable x^r_{ij} for the charging mode that takes value 1 if and only if the vehicle is running on this mode. For each arc $(i,j) \in A$, let c^r_{ij} and t^r_{ij} be the cost and travel time for the charging mode, c^b_{ij} and t^b_{ij} be the cost and travel time for the boost mode, c^f_{ij} and t^f_{ij} be the cost and travel time for the combustion mode, and c^e_{ij} and t^e_{ij} be the cost and travel time for the electric mode. For each node $i \in V$, let s_i be the service time. The charging and discharging rates of the vehicle battery are denoted by r_c and r_d, respectively. The values of all parameters can be found in Doppstadt, Koberstein, and Vigo (2016).

Then the HEV traveling salesman problem (HEV-TSP) is as follows:

$$\min \quad Z = \sum_{(i,j)\in A} c^r_{ij}x^r_{ij} + c^b_{ij}x^b_{ij} + c^f_{ij}x^f_{ij} + c^e_{ij}x^e_{ij} \tag{95}$$

$$\text{s.t.} \quad \sum_{i\in V} s_i + \sum_{(i,j)\in A} \left(x^r_{ij}t^r_{ij} + x^b_{ij}t^b_{ij} + x^f_{ij}t^f_{ij} + x^e_{ij}t^e_{ij} \right) \le T \tag{96}$$

$$y_i + \left(r_c x^r_{ij}t^r_{ij} - r_d x^b_{ij}t^b_{ij} - r_d x^e_{ij}t^e_{ij} \right) \ge y_j - (1 - x_{ij})M \qquad \forall (i,j) \in A \tag{97}$$

$$0 \le y_i \le \overline{B} \qquad \forall i \in V \tag{98}$$

$$y_0 = 0 \tag{99}$$

(8)–(11), (20).

Following the same approach as in Section 4, we can develop an energy accumulation inequality based on constraints (97):

$$y_0 + r_c \sum_{(i,j)\in A} x^r_{ij}t^r_{ij} - r_d \sum_{(i,j)\in A} \left(x^b_{ij}t^b_{ij} + x^e_{ij}t^e_{ij} \right) \ge y_{n+1}, \tag{100}$$

which can be directly added to HEV-TSP and solved by the proposed branch-and-cut algorithm. Here we refer to the model (8)–(11), (20), (95)–(100) as HEV-TSP with valid inequality (HEV-TSP-VI).

To compare our proposed model and solution method with those of Doppstadt, Koberstein, and Vigo (2016), we solve their instances. The results are shown in Table 5, where it can be seen that the energy accumulation inequality (100) can significantly improve the computation efficiency of our branch-and-cut algorithm. In addition, HEV-TSP-VI outperforms the iterated tabu search method provided by Doppstadt, Koberstein, and Vigo (2016) in two ways: (1) HEV-TSP-VI can always find the optimal value of the problem while the heuristic cannot, especially for the instances with 50 customers; (2) our algorithm achieves a faster runtime while utilizing comparable computational resources.

Table 5: Comparison with the Iterated Tabu Search method (Doppstadt, Koberstein, and Vigo 2016)

Instance	HEV-TSP			HEV-TSP-VI			Iterated Tabu Search		
α_β_π	*Obj*	*Time*	*Gap*	*Obj*	*Time*	*Gap*	*Obj*	*Time*	$Diff^*$
1_8_1	1830.69	1.9	0.00	1830.69	**0.4**	0.00	1830.69	20	0.00
1_8_2	1553.15	2.1	0.00	1553.15	**0.2**	0.00	1553.15	21	0.00
1_8_3	1435.74	3.3	0.00	1435.74	**0.7**	0.00	1435.74	22	0.00
2_8_1	7189.85	1.7	0.00	7189.85	**0.3**	0.00	7189.85	22	0.00
2_8_2	7140.95	1.2	0.00	7140.95	**0.3**	0.00	7140.95	20	0.00
2_8_3	7292.25	1.8	0.00	7292.25	**0.3**	0.00	7292.25	22	0.00
3_8_1	12706.6	1.9	0.00	12706.6	**0.3**	0.00	12706.6	20	0.00
3_8_2	12687.9	1.7	0.00	12687.9	**0.3**	0.00	12687.9	24	0.00
3_8_3	12708.57	1.4	0.00	12708.57	**0.3**	0.00	12708.57	19	0.00
1_10_1	1798.94	28.3	0.00	1798.94	**0.2**	0.00	1798.94	54	0.00
1_10_2	1598.18	54.2	0.00	1598.18	**0.5**	0.00	1598.18	53	0.00
1_10_3	1478.9	60.8	0.00	1478.9	**0.2**	0.00	1478.9	58	0.00
2_10_1	7308.15	27.4	0.00	7308.15	**0.4**	0.00	7308.15	59	0.00
2_10_2	7362.93	17.8	0.00	7362.93	**0.4**	0.00	7362.93	55	0.00
2_10_3	7290.82	16.1	0.00	7290.82	**0.3**	0.00	7290.82	70	0.00
3_10_1	12747.22	33.7	0.00	12747.22	**0.5**	0.00	12747.22	63	0.00
3_10_2	12725.88	46.0	0.00	12725.88	**0.3**	0.00	12725.88	64	0.00
3_10_3	12935.48	45.9	0.00	12935.48	**0.4**	0.00	12935.48	62	0.00
1_20_1	2005.89	7200.3	61.02	2005.89	**2.1**	0.00	2005.89	419	0.00
1_20_2	1969.78	7200.4	69.41	1969.78	**1.9**	0.00	1969.78	357	0.00
1_20_3	1606.42	7200.2	52.58	1606.42	**2.0**	0.00	1606.42	454	0.00
2_20_1	7819.22	7200.0	18.83	7807.05	**4.7**	0.00	7807.05	477	0.00
2_20_2	7671.48	7200.1	15.42	7670.94	**5.7**	0.00	7670.94	447	0.00
2_20_3	7713.39	7200.1	17.74	7709.14	**4.3**	0.00	7709.14	454	0.00
3_20_1	13343.32	7200.0	10.09	13329.82	**6.7**	0.00	13335.85	432	0.05
3_20_2	13287.61	7200.4	9.06	13287.61	**4.6**	0.00	13287.61	422	0.00
3_20_3	13247.33	7200.1	7.17	13247.33	**4.4**	0.00	13247.33	388	0.00
1_50_1	2755.28	7200.1	75.13	2712.9	**29.6**	0.00	2767.36	8218	2.01
1_50_2	2493.26	7200.1	74.91	2489.24	**39.2**	0.00	2491.45	9768	0.09
1_50_3	2509.92	7200.3	73.66	2474.21	**32.2**	0.00	2509.53	8980	1.43
2_50_1	8764.52	7200.1	38.25	8338.12	**138.9**	0.00	8397.48	10224	0.71
2_50_2	8790.33	7200.2	27.99	8425.7	**426.7**	0.00	8439.57	10623	0.16
2_50_3	8476.82	7200.1	37.23	8422.15	**304.8**	0.00	8446.29	12164	0.29
3_50_1	13901.24	7200.1	21.63	13846.98	**120.3**	0.00	13966.47	11537	0.86
3_50_2	14119.29	7200.1	21.55	13935.63	**88.1**	0.00	13953.79	11123	0.13
3_50_3	13863.99	7200.1	13.12	13805.51	**59.4**	0.00	13805.51	9661	0.00
#Opt			18			36			27

[a] Iterated Tabu Search: the objective values and computation times are from Table 6 of Doppstadt, Koberstein, and Vigo (2016) (The columns of 'Best Result');
[b] *Obj*: objective value; *Time*: computation time (s); *Gap*: optimality gap (%); $Diff^*$: percentage increase compared to HEV-TSP-VI.

6.4 The value of joint optimization

First, we compare our proposed PHEV-TSPS with some policies such as only using fuel, only using electricity, and the sequential optimization method described in Section 3.2. Results are summarized in Table 6 with details in Table 11 in Appendix D. It can be seen that our proposed PHEV-TSPS can significantly reduce energy consumption costs compared to the policy of solely using fuel. Using only electricity is impractical as the PHEV may run out of battery and fail to complete the journey. In addition, the sequential optimization method performs worse than our proposed PHEV-TSPS, resulting in over 7% more energy consumption costs in some instances.

Table 6: Comparison of PHEV-TSPS with some other policies

		Only Fuel Mode			Only Electricity Mode			Sequential Method		
$\#Cus$	$\#Ins$	$\#Opt$	$\#Inf$	$Diff$	$\#Opt$	$\#Inf$	$Diff$	$\#Opt$	$\#Inf$	$Diff$
8	9	9	0	48.42	3	6	_	9	0	1.60
10	9	9	0	48.55	3	6	_	9	0	1.55
20	9	9	0	45.52	3	6	_	9	0	0.63
Total	27	27	0	47.50	9	18	_	27	0	1.26

[a] $\#Inf$: the number of the instances that are infeasible.

Second, to assess the advantages of incorporating speed optimization in PHEV-TSPS over a PHEV-TSPS with fixed speeds, we consider a PHEV-TSPS with fixed speeds in which the PHEV is assumed to run on speeds from Table 2 of Doppstadt, Koberstein, and Vigo (2016) or on speed limits on arcs, respectively. We then solve the PHEV-TSPS with fixed speeds using the given speeds. The results are summarized in Table 7, and the details are shown in Table 12 in Appendix D.

It appears that the proposed PHEV-TSPS outperforms the TSPS with fixed speeds in terms of energy consumption cost. The use of speed values from Table 2 of Doppstadt, Koberstein, and Vigo (2016) can lead to energy consumption costs that are up to 59% higher than those obtained with the proposed model. Similarly, the use of speed limits can lead to energy consumption costs that are up to 59% higher than those obtained with the proposed model. This comparison supports the advantages of incorporating speed optimization into the TSP.

Table 7: Performance of the PHEV-TSPS with fixed speeds

		Doppstadt, Koberstein, and Vigo (2016)			Speed Limits		
$\#Cus$	$\#Ins$	$\#Opt$	$aObj(\times 10^7)$	$Diff$	$\#Opt$	$aObj(\times 10^7)$	$Diff$
8	9	9	13.42	15.59	9	14.80	41.59
10	9	9	13.69	15.37	9	15.09	36.45
20	9	9	15.27	22.43	9	16.47	33.62
Total	27	27	14.13	17.79	27	15.46	37.22

[a] $aObj$: the average objective value.

6.5 Sensitivity analysis

This section presents a sensitivity analysis of the proposed PHEV-TSPS, including the impacts of road gradient and energy recuperation, respectively.

6.5.1 Impact of the road gradient

To investigate the impact of road gradient on PHEV-TSPS, we test it on different values of this parameter. Specifically, in one set of experiments, the elevation of each node is randomly chosen from 0 to 200 meters. In another set of experiments, the elevation of each node is randomly selected from 0 to 300 meters. The results of these experiments are presented in Table 13 in Appendix D, indicating that higher road gradients can lead to increased energy consumption costs in most cases, because the PHEVs need more energy to climb the steeper road slopes.

6.5.2 Impact of energy recuperation

To investigate the impact of energy recuperation on the energy consumption cost, we force $x^r_{ij} = 0$ for all arcs, and then calculate the PHEV-TSPS under different road gradients. The results are shown in Table 14 in Appendix D.

The comparison between Tables 13–14 reveals that energy recuperation results in only a marginal reduction in energy consumption cost (less than 1%) when the maximum elevation is 100 meters. This is because PHEV cannot recuperate energy under such a small road gradient. However, when the maximum elevation is increased to 200 or 300 meters, the energy consumption cost can be reduced by more than 2.5% in some instances.

6.6 Impact of charging stations at customer locations

In this section, we aim to investigate the impact of charging stations on PHEV-TSPS. It is assumed that each customer location is equipped with a charging station that has a charging rate of 60 kilowatts. Since battery charging takes time, we set larger travel time budgets, which are 7200, 14400, and 21600 seconds for $\alpha = 1, 2, 3$, respectively.

We compare three models: PHEV-TSPS, PHEV-TSPS with charging stations (PHEV-TSPS-CS), and PHEV-TSPS-CS without fuel (PHEV-TSPS-CSwF), and present the calculation results in Table 15 in Appendix D. It can be seen that when $\alpha = 1$, all three models have the same cost as the journey can be completed using the initial battery charge. When $\alpha = 2$, PHEV-TSPS-CS and PHEV-TSPS-CSwF have lower costs than PHEV-TSPS as they do not use fuel during the journey. This is because electricity has a lower cost than fuel, and the former two models recharge the battery during the journey. When $\alpha = 3$, PHEV-TSPS-CSwF cannot have a feasible solution as the initial battery charge cannot cover the path between the depot and the first customer.

7 Conclusions

This paper presents a PHEV TSP with speed optimization that jointly optimizes speed, route, and operation modes to minimize the energy consumption cost over a journey. The problem is formulated as two mixed-integer nonlinear programming models, one with continuous speed and the other with discretized speed. To solve the two models efficiently, the paper proposes valid inequalities to strengthen them and linearizes them to MILP models, which are then solved by a branch-and-cut algorithm. The computational experiments demonstrate that the proposed methods can optimally solve instances with a realistic number of customers within a reasonable time, making them applicable to daily tour planning problems. Furthermore, the proposed models and solution methods can also be utilized for HEVs, and solve the problem optimally with high efficiency compared to existing methods. The experiments indicate that the joint optimization method outperforms the sequential optimization method and models with fixed speeds in energy consumption cost, thereby validating the importance of incorporating speed optimization into routing planning problems for PHEVs. Additionally, numerical experiments show that charging stations can help reduce the energy consumption cost.

This research warrants some future investigations. First, as vehicles running on roads are bound by uncertain traffic speeds (Wu et al. 2021), it would be valuable to incorporate traffic speed uncertainty into the proposed models, making them more practical. Second, considering the existence of different paths between customers, each with features such as distance, speed limit, and other factors (Huang et al. 2017), incorporating path selection into the model will make the problem more flexible.

Appendix A PHEV-TSPS with charging stations

This appendix shows how our approach can be applied to cases where charging stations are not limited to customer locations.

To model the recharging opportunities during the journey, we refer to the method proposed by Roberti and Wen (2016) for the case of an electric vehicle fleet and define the recharging path between nodes i and j that involves visiting one charging station. Here, we adopt a full-recharge policy where the battery is charged to its full capacity upon visiting the charging station. Moreover, we assume that the stopping time at the charging station is constant (Andelmin and Bartolini 2017; Bruglieri et al. 2019).

Let d^*_{ij} denote the distance of the recharging path between nodes i and j, and d'_{ij} denote the distance between node i and the charging station. For each arc $(i, j) \in A$, let x^{f*}_{ij} be a binary variable that takes value 1 if and only if the vehicle is operating on the fuel mode on the recharging path, x^{e*}_{ij} be a binary variable that takes the value 1 if and only if the vehicle is operating on the electric mode on the recharging path, x^{b*}_{ij} be a binary variable that takes the value 1 if and only if the vehicle is operating on the boost mode on the recharging path, and x^{r*}_{ij} be a binary variable that takes the value 1 if and only if the vehicle is operating on the energy recuperation mode on the recharging path. We also let y_{ij} and t^* be the state of charge and stopping time at a charging station, respectively. Then the PHEV-TSPS with charging stations can be formulated as follows:

$$\min \quad Z = \sum_{(i,j)\in A} \left(c_f x^f_{ij} + c_e x^e_{ij} + c_b x^b_{ij}\right) E_{ij} - c_e x^r_{ij}(y_j - y_i) + \left(c_f x^{f*}_{ij} + c_e x^{e*}_{ij} + c_b x^{b*}_{ij}\right) E^*_{ij} - c_e x^{r*}_{ij}(y_j - y_i - \overline{B} + y_{ij}) \tag{101}$$

$$\text{s.t.} \quad E^*_{ij} = \left(\frac{1}{\eta_d} - \eta_g\right) d^*_{ij} \max\left\{mg\sin\theta_{ij} + \frac{1}{2}C_d\rho A v^2_{ij} + C_r mg\cos\theta_{ij}, 0\right\} + \eta_g d^*_{ij}\left(mg\sin\theta_{ij} + \frac{1}{2}C_d\rho A v^2_{ij} + C_r mg\cos\theta_{ij}\right) \quad \forall (i,j)\in A \tag{102}$$

$$x^f_{ij} + x^e_{ij} + x^b_{ij} + x^r_{ij} + x^{f*}_{ij} + x^{e*}_{ij} + x^{b*}_{ij} + x^{r*}_{ij} = x_{ij} \quad \forall (i,j)\in A \tag{103}$$

$$(x^{f*}_{ij} + x^{e*}_{ij} + x^{b*}_{ij} - 1)M^*_{ij} \le E^*_{ij} \quad \forall (i,j)\in A \tag{104}$$

$$(1 - x^{r*}_{ij})M^*_{ij} \ge E^*_{ij} \quad \forall (i,j)\in A \tag{105}$$

$$\sum_{(i,j)\in A} (x^f_{ij} + x^e_{ij} + x^b_{ij} + x^r_{ij})\frac{d_{ij}}{v_{ij}} + (x^{f*}_{ij} + x^{e*}_{ij} + x^{b*}_{ij} + x^{r*}_{ij})\left(\frac{d^*_{ij}}{v_{ij}} + t^*\right) \le T \tag{106}$$

$$y_i - \left(x^e_{ij} + \mu x^b_{ij} + x^r_{ij}\right) E_{ij} - \left(x^{e*}_{ij} + \mu x^{b*}_{ij} + x^{r*}_{ij}\right) E^*_{ij} + (x^{f*}_{ij} + x^{e*}_{ij} + x^{b*}_{ij} + x^{r*}_{ij})(\overline{B} - y_{ij}) \ge y_j - (1 - x_{ij})\overline{B} \quad \forall (i,j)\in A \tag{107}$$

$$y_i - \left(x^e_{ij} + \mu x^b_{ij}\right) E_{ij} - \left(x^{e*}_{ij} + \mu x^{b*}_{ij}\right) E^*_{ij} + (x^{f*}_{ij} + x^{e*}_{ij} + x^{b*}_{ij} + x^{r*}_{ij})(\overline{B} - y_{ij}) \le y_j + (1 - x_{ij})\overline{B} \quad \forall (i,j)\in A \tag{108}$$

$$E'_{ij} = \left(\frac{1}{\eta_d} - \eta_g\right) d'_{ij} \max\left\{mg\sin\theta_{ij} + \frac{1}{2}C_d\rho A v^2_{ij} + C_r mg\cos\theta_{ij}, 0\right\} + \eta_g d'_{ij}\left(mg\sin\theta_{ij} + \frac{1}{2}C_d\rho A v^2_{ij} + C_r mg\cos\theta_{ij}\right) \quad \forall (i,j)\in A \tag{109}$$

$$y_i - (x^{e*}_{ij} + \mu x^{b*}_{ij} + x^{r*}_{ij})E'_{ij} = y_{ij} \quad \forall (i,j)\in A \tag{110}$$

$$y_{ij} \ge \underline{B} \quad \forall (i,j)\in A \tag{111}$$

$$x^{f*}_{ij}, x^{e*}_{ij}, x^{b*}_{ij}, x^{r*}_{ij} \in \{0,1\} \quad \forall (i,j)\in A \tag{112}$$

(9)–(13), (17)–(20).

Objective function (101) minimizes the total cost of energy consumption and recharging over the entire trip. The first two terms are the same as in objective function (6), while the third and fourth terms calculate the energy consumption cost over the recharging path. Constraints (102) calculate the energy consumption over each recharging path. Constraints (103) ensure that the PHEV can only run in one mode and one path on each arc. Constraints (104)–(105) are counterparts to constraints (12)–(13) on the recharging path. Constraint (106) is the travel time constraint, where the second term calculates the travel time on the recharging path. Constraints (107)–(108) are the battery flow constraints. Constraints (109) calculate the energy consumption between the start point and the charging station on each arc. Constraints (110) calculate the state of charge when the vehicle visits the charging station, and constraints (111) require that the state of charge cannot be lower than the lower bound.

The above model is more complex due to the incorporation of four extra binary variables in the recharging path, rendering it intractable for the proposed method. During our tests, we were able to solve all instances with 10 customers within 2 hours, but we were unable to solve all instances with 20 customers within the same time frame. The complexity of the model would require more tailored algorithms, which are beyond the scope of this paper.

Appendix B Proof of Lemma and Propositions

Proof of Lemma 1: Due to constraints (15), we have the inequality $x^r_{ij}(y_i - y_j) \geq x^r_{ij}E_{ij}$. Since the objective function (6) is a minimization, $x^r_{ij}(y_i - y_j)$ is minimized, making the left-hand side of the inequality as small as possible. Therefore, we have $x^r_{ij}(y_i - y_j) = x^r_{ij}E_{ij}$, and the lemma is proven. □

Proof of Proposition 1: First, it can be seen that the optimal solution of *Step 1* and *Step 2* is feasible for the PHEV-TSPS, because *Step 1* and *Step 2* contain all constraints of the PHEV-TSPS. To illustrate that *Step 1* and PHEV-TSPS can result in different speeds and routes, we can consider the following two cases:

- Assuming that the optimal routes of *Step 1* and PHEV-TSPS are the same, denoted as A^*, then the objective function (21) in *Step 1* is as follows:

$$\min \sum_{(i,j)\in A^*} E_{ij}, \tag{113}$$

  the objective function (6) in the PHEV-TSPS is as follows:

$$\begin{aligned} \min \quad & \sum_{(i,j)\in A^*} \left(c_f x^f_{ij} + c_e x^e_{ij} + c_b x^b_{ij}\right) E_{ij} - c_e x^r_{ij}(y_j - y_i) \\ \text{s.t.} \quad & x^f_{ij} + x^e_{ij} + x^b_{ij} + x^r_{ij} = 1 \qquad \forall (i,j) \in A^*. \end{aligned} \tag{114}$$

  From the above, it can be seen that the objective functions of *Step 1* and PHEV-TSPS may have different energy consumption coefficients on each arc, leading to different speed decisions.

- Similarly, assuming a fixed running speed on each arc, the energy consumption on each arc resulting from the sequential optimization method would be the same as that of PHEV-TSPS. However, the objective functions of *Step 1* and PHEV-TSPS may still differ due to the variation in energy consumption coefficients on each arc in the latter. As a result, different route decisions can be made.

Second, *Step 2* can be seen as PHEV-TSPS with fixed route and speeds, so PHEV-TSPS is a relaxed problem of *Step 2* and thus has an objective value lower than or equal to *Step 2*. □

Proof of Propositions 2 and 3: First, to solve the model (38)–(41), we write a dual formulation as follows:

$$\max_{\psi_1,\psi_2} \quad (-y_0 + y_{n+1} + \sum_{(i,j)\in A} x^r_{ij}E_{ij})\psi_1 + \sum_{(i,j)\in A}(x_{ij}E_{ij} - x^r_{ij}E_{ij})\psi_2 + c_e \sum_{(i,j)\in A} x^r_{ij}E_{ij} \tag{115}$$

$$\text{s.t.} \quad -\psi_1 + \psi_2 \le c_e \tag{116}$$

$$\psi_2 \le c_f \tag{117}$$

$$-\mu\psi_1 + \psi_2 \le c_b \tag{118}$$

$$\psi_1 \ge 0. \tag{119}$$

Then, we solve the problem (115)–(119) by two cases:

(a) If $\frac{c_f - c_b}{\mu} \le c_f - c_e$, the feasible region of model (115)–(119) is the cyan area of Figure 2. When $\frac{y_0 - y_{n+1} - \sum_{(i,j)\in A} x^r_{ij}E_{ij}}{\sum_{(i,j)\in A} x_{ij}E_{ij} - x^r_{ij}E_{ij}} \ge 1$, the optimal solution is $(0, c_e)$, the optimal value is $c_e \sum_{(i,j)\in A} x_{ij}E_{ij}$; when $\frac{y_0 - y_{n+1} - \sum_{(i,j)\in A} x^r_{ij}E_{ij}}{\sum_{(i,j)\in A} x_{ij}E_{ij} - x^r_{ij}E_{ij}} < 1$, the optimal solution is $(\frac{c_b - c_e}{1-\mu}, \frac{c_b - \mu c_e}{1-\mu})$, the optimal value is $\frac{1}{1-\mu}\Big((c_e - c_b)(y_0 - y_{n+1} - \sum_{(i,j)\in A} x^r_{ij}E_{ij}) + (c_b - \mu c_e)\sum_{(i,j)\in A}(x_{ij}E_{ij} - x^r_{ij}E_{ij})\Big) + c_e \sum_{(i,j)\in A} x^r_{ij}E_{ij}$.

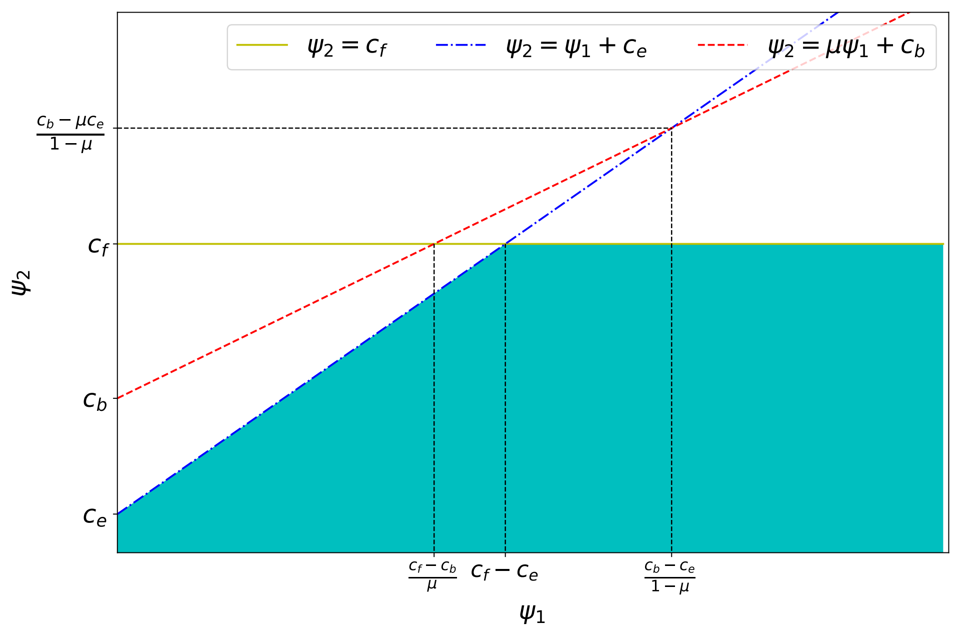

Figure 2: Feasible area of model (115)–(119) $\left(\frac{c_f - c_b}{\mu} \le c_f - c_e\right)$

(b) If $\frac{c_f - c_b}{\mu} > c_f - c_e$, the feasible region of model (115)–(119) is the cyan area of Figure 3. When $\frac{y_0 - y_{n+1} - \sum_{(i,j)\in A} x^r_{ij}E_{ij}}{\sum_{(i,j)\in A} x_{ij}E_{ij} - x^r_{ij}E_{ij}} \ge 1$, the optimal solution is $(0, c_e)$, the optimal value is $c_e \sum_{(i,j)\in A} x_{ij}E_{ij}$. When $\mu \le \frac{y_0 - y_{n+1} - \sum_{(i,j)\in A} x^r_{ij}E_{ij}}{\sum_{(i,j)\in A} x_{ij}E_{ij} - x^r_{ij}E_{ij}} \le 1$, the optimal solution is $(\frac{c_b - c_e}{1-\mu}, \frac{c_b - \mu c_e}{1-\mu})$, the optimal value is $\frac{1}{1-\mu}\Big((c_e - c_b)(y_0 - y_{n+1} - \sum_{(i,j)\in A} x^r_{ij}E_{ij}) + (c_b - \mu c_e)\sum_{(i,j)\in A}(x_{ij}E_{ij} - x^r_{ij}E_{ij})\Big) + c_e \sum_{(i,j)\in A} x^r_{ij}E_{ij}$. When $\frac{y_0 - y_{n+1} - \sum_{(i,j)\in A} x^r_{ij}E_{ij}}{\sum_{(i,j)\in A} x_{ij}E_{ij}} \le \mu$, the optimal solution is $\left(\frac{c_f - c_b}{\mu}, c_f\right)$, the optimal value is $\frac{(c_b - c_f)(y_0 - y_{n+1} - \sum_{(i,j)\in A} x^r_{ij}E_{ij})}{\mu} + c_f \sum_{(i,j)\in A}(x_{ij}E_{ij} - x^r_{ij}E_{ij}) + c_e \sum_{(i,j)\in A} x^r_{ij}E_{ij}$.

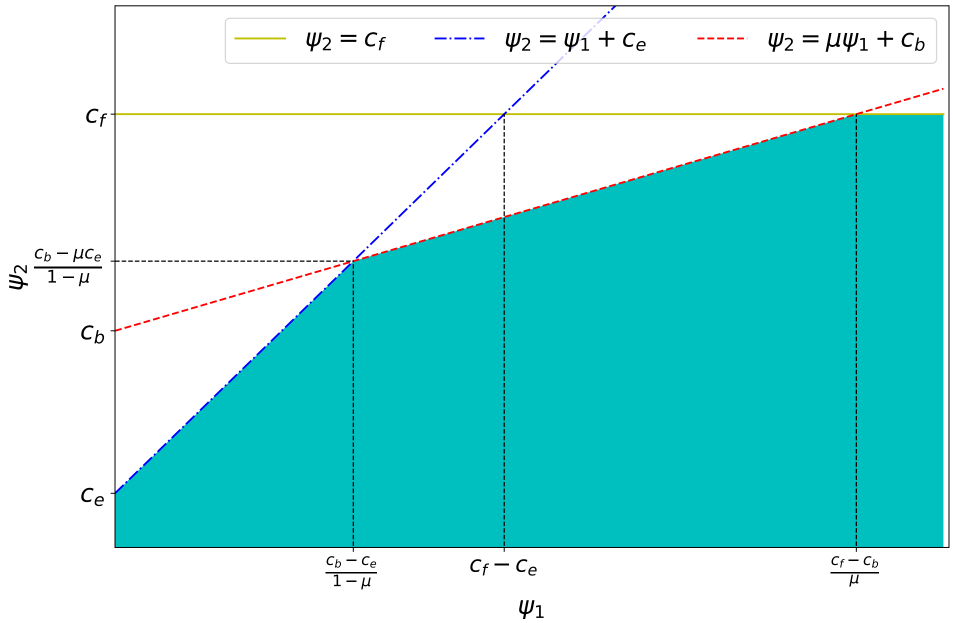

Figure 3: Feasible area of model (115)–(119) $\left(\frac{c_f - c_b}{\mu} \geq c_f - c_e\right)$

Second, in order to integrate the lower bound calculated by model (115)–(119) with PHEV-TSPS, we use the multiple choice model (Croxton, Gendron, and Magnanti 2003) to combine the objective values under different cases:

(a) If $\frac{c_f - c_b}{\mu} \leq c_f - c_e$, we introduce two new continuous variables, κ_1 and κ_2, and two new binary variables, δ_1 and δ_2, then the optimal value of model (38)–(41) or model (115)–(119) can be calculated by the following function:

$$\underline{Z}_a = c_e\kappa_1 + \frac{(y_0 - y_{n+1} - \sum_{(i,j)\in A} x_{ij}^r E_{ij})(c_e - c_b)}{1-\mu}\delta_2 + \frac{c_b - \mu c_e}{1-\mu}\kappa_2 + c_e \sum_{(i,j)\in A} x_{ij}^r E_{ij} \tag{120}$$

subject to constraints (43)–(47);

(b) If $\frac{c_f - c_b}{\mu} > c_f - c_e$, we introduce three new continuous variables, κ_1, κ_2 and κ_3, and three new binary variables, δ_1, δ_2 and δ_3, then the optimal value of model (38)–(41) or model (115)–(119) can be calculated by the function

$$\begin{aligned}\underline{Z}_b = c_e\kappa_1 &+ \frac{(y_0 - y_{n+1} - \sum_{(i,j)\in A} x_{ij}^r E_{ij})(c_e - c_b)}{1-\mu}\delta_2 + \frac{c_b - \mu c_e}{1-\mu}\kappa_2 \\ &+ \frac{(y_0 - y_{n+1} - \sum_{(i,j)\in A} x_{ij}^r E_{ij})(c_b - c_f)}{1-\mu}\delta_3 + c_f\kappa_3 + c_e \sum_{(i,j)\in A} x_{ij}^r E_{ij}\end{aligned} \tag{121}$$

subject to constraints (49)–(54).

Finally, we can obtain the following valid inequalities under two cases. If $\frac{c_f - c_b}{\mu} \geq c_f - c_e$, the following inequalities are valid to PHEV-TSPS:

$$Z \geq \underline{Z}_a \tag{122}$$

$$(43)\text{–}(47), (120).$$

Thus Proposition 2 is proved.

If $\frac{c_f - c_b}{\mu} \leq c_f - c_e$, the following inequalities are valid to PHEV-TSPS:

$$Z \geq \underline{Z}_b \tag{123}$$

(49)–(54), (121).

Thus Proposition 3 is proved. □

Appendix C Solution method for PHEV-TSPS-CS

This appendix presents the modifications made to the solution method proposed in Section 5 when applied to PHEV-TSPS-CS.

First, constraints (31)–(33) can be reformulated to the follows:

$$\sum_{(i,j)\in A} d_{ij} q_{ij} + \sum_{i\in V} \tau_i \leq T \tag{124}$$

$$y_i - w^e_{ij} - \mu w^b_{ij} - w^r_{ij} + \epsilon\tau_i \geq y_j - (1 - x_{ij})\overline{B} \qquad \forall (i,j) \in A \tag{125}$$

$$y_i - w^e_{ij} - \mu w^b_{ij} + \epsilon\tau_i \leq y_j + (1 - x_{ij})\overline{B} \qquad \forall (i,j) \in A \tag{126}$$

(62)–(63).

Second, energy accumulation inequality (36) can be linearized to the follows:

$$\sum_{(i,j)\in A} (w^e_{ij} + \mu w^b_{ij} + w^r_{ij}) \leq y_0 - y_{n+1} + \epsilon \sum_{i\in V} \tau_i. \tag{127}$$

Third, if $\frac{c_f - c_b}{\mu} \leq c_f - c_e$, we can formulate the lower bound inequalities for PHEV-TSPS-CS as follows, similar to Proposition 2:

$$Z \geq c_e\kappa_1 + \frac{(y_0 - y_{n+1} + \epsilon\sum_{i\in V}\tau_i - \sum_{(i,j)\in A} x^r_{ij}E_{ij})(c_e - c_b)}{1-\mu}\delta_2 + \frac{c_b - \mu c_e}{1-\mu}\kappa_2 + c_e \sum_{(i,j)\in A} x^r_{ij}E_{ij} \tag{128}$$

$$\kappa_1 \leq (y_0 - y_{n+1} + \epsilon \sum_{i\in V}\tau_i - \sum_{(i,j)\in A} x^r_{ij}E_{ij})\delta_1 \tag{129}$$

$$(y_0 - y_{n+1} + \epsilon \sum_{i\in V}\tau_i - \sum_{(i,j)\in A} x^r_{ij}E_{ij})\delta_2 \leq \kappa_2 \leq M\delta_2 \tag{130}$$

(43), (46)–(47),

where constraints (128)–(130) can be linearized to the following constraints:

$$\sigma_1 \leq y_0 - y_{n+1} + \epsilon \sum_{i\in V}\tau_i - \sum_{(i,j)\in A} w^r_{ij} + (1-\delta_2)M^* \tag{131}$$

$$\kappa_1 \leq y_0 - y_{n+1} + \epsilon \sum_{i\in V}\tau_i - \sum_{(i,j)\in A} w^r_{ij} + (1-\delta_1)M^* \tag{132}$$

$$\kappa_2 \geq y_0 - y_{n+1} + \epsilon \sum_{i\in V}\tau_i - \sum_{(i,j)\in A} w^r_{ij} - (1-\delta_2)M^* \tag{133}$$

(78)–(81), (83).

Finally, if $\frac{c_f - c_b}{\mu} > c_f - c_e$, we can formulate the lower bound inequalities for PHEV-TSPS-CS as follows, similar to Proposition 3:

$$Z \geq c_e\kappa_1 + \frac{(y_0 - y_{n+1} + \epsilon\sum_{i\in V}\tau_i - \sum_{(i,j)\in A} x^r_{ij}E_{ij})(c_e - c_b)}{1-\mu}\delta_2 + \frac{c_b - \mu c_e}{1-\mu}\kappa_2$$

$$+\frac{(y_0 - y_{n+1} + \epsilon \sum_{i\in V} \tau_i - \sum_{(i,j)\in A} x^r_{ij} E_{ij})(c_b - c_f)}{1-\mu}\delta_3 + c_f\kappa_3 + c_e \sum_{(i,j)\in A} x^r_{ij} E_{ij} \tag{134}$$

$$\kappa_1 \le (y_0 - y_{n+1} + \epsilon \sum_{i\in V} \tau_i - \sum_{(i,j)\in A} x^r_{ij} E_{ij})\delta_1 \tag{135}$$

$$(y_0 - y_{n+1} + \epsilon \sum_{i\in V} \tau_i - \sum_{(i,j)\in A} x^r_{ij} E_{ij})\delta_2 \le \kappa_2 \le \frac{(y_0 - y_{n+1} + \epsilon \sum_{i\in V} \tau_i - \sum_{(i,j)\in A} x^r_{ij} E_{ij})\delta_2}{\mu} \tag{136}$$

$$\frac{(y_0 - y_{n+1} + \epsilon \sum_{i\in V} \tau_i - \sum_{(i,j)\in A} x^r_{ij} E_{ij})\delta_3}{\mu} \le \kappa_3 \le M\delta_3 \tag{137}$$

(49), (53)–(54),

where constraints (134)–(137) can be linearized to the following constraints:

$$\sigma_2 \le y_0 - y_{n+1} + \epsilon \sum_{i\in V} \tau_i - \sum_{(i,j)\in A} w^r_{ij} + (1-\delta_3)M^* \tag{138}$$

$$\kappa_1 \le y_0 - y_{n+1} + \epsilon \sum_{i\in V} \tau_i - \sum_{(i,j)\in A} w^r_{ij} + (1-\delta_1)M^* \tag{139}$$

$$y_0 - y_{n+1} + \epsilon \sum_{i\in V} \tau_i - \sum_{(i,j)\in A} w^r_{ij} - (1-\delta_2)M^* \le \kappa_2$$
$$\le \frac{(y_0 - y_{n+1} + \epsilon \sum_{i\in V} \tau_i - \sum_{(i,j)\in A} w^r_{ij} + (1-\delta_2) * M^*)}{\mu} \tag{140}$$

$$\mu\kappa_3 \ge y_0 - y_{n+1} + \epsilon \sum_{i\in V} \tau_i - \sum_{(i,j)\in A} w^r_{ij} - (1-\delta_3)M^* \tag{141}$$

(78), (86)–(89), (91), (93), (131).

Appendix D Results of the experiments

Table 8: Performances of the solution methods for PHEV-TSPS

Instance	*Original*			*LB*			*EAI*			*LB + EAI*			*LB + EAI + BP*		
α_β_π	$Obj(\times 10^7)$	*Time*	*Gap*	$Obj(\times 10^7)$	*Time*	*Gap*	$Obj(\times 10^7)$	*Time*	*Gap*	$Obj(\times 10^7)$	*Time*	*Gap*	$Obj(\times 10^7)$	*Time*	*Gap*
1_8_1	1.602	**0.5**	0.00	1.602	0.9	0.00	1.602	**0.5**	0.00	1.602	**0.5**	0.00	1.602	0.7	0.00
1_8_2	1.443	**0.3**	0.00	1.443	**0.3**	0.00	1.443	0.4	0.00	1.443	0.4	0.00	1.443	0.6	0.00
1_8_3	1.139	**0.3**	0.00	1.139	0.4	0.00	1.139	0.4	0.00	1.139	**0.3**	0.00	1.139	0.5	0.00
2_8_1	9.707	10.3	0.00	9.707	2.4	0.01	9.707	1.3	0.01	9.707	1.5	0.01	9.707	**1.2**	0.00
2_8_2	10.269	18.7	0.00	10.269	1.9	0.00	10.269	2.2	0.00	10.269	**1.8**	0.00	10.269	**1.8**	0.00
2_8_3	9.844	15.3	0.00	9.844	**1.3**	0.00	9.844	1.5	0.00	9.844	1.4	0.00	9.844	1.6	0.00
3_8_1	21.698	4.1	0.00	21.698	1.8	0.00	21.698	**1.5**	0.00	21.698	1.9	0.00	21.698	1.8	0.00
3_8_2	21.930	10.4	0.00	21.930	1.9	0.00	21.930	2.0	0.00	21.930	2.1	0.00	21.930	**1.8**	0.00
3_8_3	22.038	7.7	0.00	22.038	**1.6**	0.00	22.038	**1.6**	0.00	22.038	2.1	0.00	22.038	2.0	0.00
1_10_1	1.814	**0.6**	0.00	1.814	1.6	0.00	1.814	1.1	0.00	1.814	0.8	0.00	1.814	0.8	0.00
1_10_2	1.754	**0.5**	0.00	1.754	0.8	0.00	1.754	0.8	0.00	1.754	**0.5**	0.00	1.754	0.6	0.00
1_10_3	1.671	1.3	0.00	1.671	1.1	0.00	1.671	1.1	0.00	1.671	**0.9**	0.00	1.671	1.6	0.00
2_10_1	10.132	619.9	0.00	10.132	2.6	0.01	10.132	**2.1**	0.00	10.132	2.7	0.00	10.132	2.3	0.00
2_10_2	10.438	403.0	0.00	10.438	2.7	0.00	10.439	3.0	0.01	10.438	**2.0**	0.00	10.438	2.9	0.00
2_10_3	10.162	613.6	0.00	10.162	3.4	0.00	10.162	**1.4**	0.01	10.162	2.6	0.00	10.162	1.8	0.00
3_10_1	21.654	26.0	0.00	21.654	**3.0**	0.00	21.654	3.1	0.00	21.654	3.4	0.00	21.654	3.2	0.00
3_10_2	21.601	117.2	0.00	21.603	3.1	0.01	21.602	2.5	0.00	21.601	2.4	0.00	21.601	**2.2**	0.00
3_10_3	22.699	48.2	0.00	22.699	4.0	0.00	22.699	2.8	0.00	22.699	2.6	0.00	22.699	**2.2**	0.00
1_20_1	2.760	108.6	0.00	2.760	53.1	0.00	2.760	**4.1**	0.00	2.760	5.0	0.01	2.760	9.5	0.00
1_20_2	2.377	3.0	0.00	2.377	**2.5**	0.00	2.377	3.7	0.00	2.377	3.0	0.00	2.377	3.4	0.00
1_20_3	2.162	64.6	0.00	2.162	4.4	0.00	2.162	**3.3**	0.00	2.162	5.1	0.00	2.162	14.8	0.00
2_20_1	12.934	7200.1	35.24	12.934	36.7	0.00	12.934	37.5	0.00	12.934	**29.2**	0.01	12.934	42.0	0.00
2_20_2	12.415	7200.1	33.11	12.415	48.1	0.00	12.415	**28.8**	0.01	12.415	39.2	0.00	12.415	39.7	0.00
2_20_3	12.533	7200.2	34.36	12.533	43.7	0.00	12.533	32.4	0.00	12.533	30.4	0.00	12.533	**29.5**	0.00
3_20_1	24.556	7200.1	10.06	24.556	50.9	0.00	24.556	39.4	0.00	24.556	31.8	0.00	24.556	**30.3**	0.00
3_20_2	24.468	7200.1	8.94	24.468	57.5	0.00	24.468	60.0	0.00	24.468	**42.1**	0.00	24.468	45.6	0.00
3_20_3	24.205	7200.1	8.43	24.205	41.8	0.00	24.205	**35.4**	0.00	24.205	39.5	0.00	24.205	46.5	0.00
1_30_1	3.075	7200.1	2.91	3.075	224.8	0.00	3.075	**24.4**	0.01	3.075	52.6	0.01	3.075	44.6	0.00
1_30_2	2.441	53.9	0.00	2.441	**8.5**	0.00	2.441	9.5	0.00	2.441	8.6	0.00	2.441	21.9	0.00
1_30_3	3.359	7200.1	7.62	3.359	264.6	0.00	3.359	**49.4**	0.00	3.359	59.9	0.00	3.359	159.5	0.00
2_30_1	13.782	7200.1	36.44	13.768	2598.4	0.00	13.768	**107.3**	0.00	13.768	130.6	0.00	13.768	127.2	0.00
2_30_2	14.084	7200.1	37.15	13.826	4621.9	0.00	13.826	**256.2**	0.00	13.826	421.8	0.00	13.826	842.4	0.00
2_30_3	13.890	7200.1	37.77	13.890	1529.5	0.00	13.890	182.5	0.00	13.890	**103.5**	0.01	13.890	208.0	0.00
3_30_1	26.736	7200.1	19.81	26.567	6107.1	0.00	26.567	159.8	0.00	26.567	187.4	0.00	26.567	**144.6**	0.00
3_30_2	27.485	7200.6	22.32	26.755	7200.1	1.19	26.755	5001.9	0.00	26.755	2268.6	0.00	26.756	**266.6**	0.01
3_30_3	25.895	7200.1	13.43	25.723	1223.0	0.01	25.725	186.5	0.01	25.723	163.1	0.00	25.725	**126.7**	0.01
Average	12.251	2859.2	8.54	12.484	670.9	0.03	12.484	173.7	0.00	12.484	101.4	0.00	12.484	**62.0**	0.00

Table 9: Performances of PHEV-TSPS-VI and PHEV-TSPSD-VI (Part 1)

Instance	PHEV-TSPS-VI			Speed Discretization												
				0.1 (m/s)				0.3 (m/s)				0.5 (m/s)				
α_β_π	Obj $(\times 10^7)$	$Time$	Gap	Obj_1 $(\times 10^7)$	$Time$	Gap	$\frac{Obj_1}{Obj}$	Obj_2 $(\times 10^7)$	$Time$	Gap	$\frac{Obj_3}{Obj}$	Obj_3 $(\times 10^7)$	$Time$	Gap	$\frac{Obj_3}{Obj}$
1_8_1	**1.602**	0.7	0.00	**1.602**	0.5	0.01	1.000	1.603	0.2	0.01	1.000	1.603	0.2	0.01	1.000
1_8_2	**1.443**	0.6	0.00	**1.443**	0.8	0.01	1.000	**1.443**	0.3	0.00	1.000	**1.443**	0.4	0.00	1.000
1_8_3	**1.139**	0.5	0.00	**1.139**	1.4	0.00	1.000	**1.139**	0.2	0.00	1.000	**1.139**	0.2	0.00	1.000
2_8_1	**9.707**	1.2	0.00	9.709	1.0	0.01	1.000	9.711	0.6	0.01	1.000	9.714	1.1	0.00	1.001
2_8_2	**10.269**	1.8	0.00	10.288	3.3	0.00	1.002	10.304	2.2	0.00	1.003	10.296	1.0	0.00	1.003
2_8_3	**9.844**	1.6	0.00	9.845	0.7	0.01	1.000	9.847	0.6	0.00	1.000	9.855	0.5	0.01	1.001
3_8_1	**21.698**	1.8	0.00	21.703	3.2	0.00	1.000	21.713	1.1	0.00	1.001	21.730	1.5	0.00	1.001
3_8_2	**21.930**	1.8	0.00	21.934	2.5	0.00	1.000	21.938	1.8	0.00	1.000	21.974	1.5	0.01	1.002
3_8_3	**22.038**	2.0	0.00	22.058	2.4	0.00	1.001	22.090	1.6	0.00	1.002	22.073	1.6	0.00	1.002
1_10_1	**1.814**	0.8	0.00	**1.814**	2.1	0.00	1.000	**1.814**	0.4	0.00	1.000	1.815	0.5	0.01	1.001
1_10_2	**1.754**	0.6	0.00	**1.754**	1.0	0.01	1.000	**1.754**	0.7	0.01	1.000	**1.754**	0.5	0.00	1.000
1_10_3	**1.671**	1.6	0.00	**1.671**	4.2	0.00	1.000	**1.671**	1.8	0.00	1.000	**1.671**	1.2	0.00	1.000
2_10_1	**10.132**	2.3	0.00	10.133	5.4	0.00	1.000	10.136	1.2	0.00	1.000	10.138	1.1	0.01	1.001
2_10_2	**10.438**	2.9	0.00	10.439	1.7	0.00	1.000	10.440	1.8	0.01	1.000	10.440	1.5	0.00	1.000
2_10_3	**10.162**	1.8	0.00	**10.162**	5.2	0.00	1.000	10.163	0.5	0.00	1.000	10.169	1.7	0.01	1.001
3_10_1	**21.654**	3.2	0.00	21.669	4.0	0.01	1.001	21.710	0.9	0.01	1.003	21.705	0.6	0.00	1.002
3_10_2	**21.601**	2.2	0.00	21.602	6.1	0.00	1.000	21.606	2.2	0.00	1.000	21.606	1.3	0.01	1.000
3_10_3	**22.699**	2.2	0.00	22.701	5.1	0.01	1.000	22.714	3.3	0.00	1.001	22.713	3.2	0.01	1.001
1_20_1	**2.760**	9.5	0.00	**2.760**	83.1	0.01	1.000	2.761	106.7	0.01	1.000	2.761	27.2	0.01	1.000
1_20_2	**2.377**	3.4	0.00	**2.377**	10.8	0.00	1.000	**2.377**	8.2	0.00	1.000	**2.377**	3.7	0.00	1.000
1_20_3	**2.162**	14.8	0.00	**2.162**	48.8	0.00	1.000	**2.162**	20.6	0.00	1.000	2.163	12.1	0.00	1.000
2_20_1	**12.934**	42.0	0.00	12.936	42.2	0.01	1.000	12.938	22.9	0.01	1.000	12.949	15.0	0.01	1.001
2_20_2	**12.415**	39.7	0.00	12.416	106.0	0.00	1.000	12.420	24.7	0.01	1.000	12.422	18.0	0.01	1.001
2_20_3	**12.533**	29.5	0.00	12.534	123.6	0.00	1.000	12.538	62.2	0.01	1.000	12.536	46.3	0.01	1.000
3_20_1	**24.556**	30.3	0.00	24.558	42.1	0.00	1.000	24.560	14.4	0.00	1.000	24.574	17.1	0.01	1.001
3_20_2	**24.468**	45.6	0.00	24.484	101.4	0.01	1.001	24.530	43.6	0.00	1.003	24.598	30.4	0.01	1.005
3_20_3	**24.205**	46.5	0.00	24.207	92.4	0.01	1.000	24.229	37.3	0.01	1.001	24.223	24.5	0.01	1.001
1_30_1	**3.075**	44.6	0.00	**3.075**	182.4	0.00	1.000	3.076	104.1	0.00	1.000	3.077	78.0	0.00	1.001
1_30_2	**2.441**	21.9	0.00	**2.441**	187.7	0.01	1.000	2.442	92.6	0.00	1.000	2.442	54.6	0.00	1.001
1_30_3	**3.359**	159.5	0.00	**3.359**	201.8	0.00	1.000	3.361	108.0	0.01	1.001	3.363	81.0	0.01	1.001

Table 9 – continued from previous page

Instance	PHEV-TSPS-VI			Speed Discretization											
				0.1 (m/s)				0.3 (m/s)				0.5 (m/s)			
α_β_π	Obj $(\times 10^7)$	$Time$	Gap	Obj_1 $(\times 10^7)$	$Time$	Gap	$\frac{Obj_1}{Obj}$	Obj_2 $(\times 10^7)$	$Time$	Gap	$\frac{Obj_3}{Obj}$	Obj_3 $(\times 10^7)$	$Time$	Gap	$\frac{Obj_3}{Obj}$
2_30_1	**13.768**	127.2	0.00	13.769	259.5	0.00	1.000	13.773	107.2	0.01	1.000	13.776	51.9	0.00	1.001
2_30_2	**13.826**	842.4	0.00	13.829	268.1	0.01	1.000	13.833	74.3	0.01	1.000	13.842	55.5	0.01	1.001
2_30_3	**13.890**	208.0	0.00	**13.890**	287.7	0.00	1.000	13.896	91.2	0.01	1.000	13.896	73.8	0.01	1.000
3_30_1	**26.567**	144.6	0.00	26.573	241.7	0.00	1.000	26.578	111.7	0.01	1.000	26.660	100.8	0.01	1.003
3_30_2	**26.756**	266.6	0.01	26.772	198.7	0.00	1.001	26.817	126.1	0.01	1.002	26.785	75.2	0.00	1.001
3_30_3	**25.725**	126.7	0.01	25.734	228.5	0.00	1.000	25.776	61.9	0.00	1.002	25.780	34.9	0.01	1.002
1_40_1	**4.296**	119.3	0.00	4.297	508.1	0.00	1.000	4.299	229.7	0.01	1.001	4.303	132.2	0.01	1.001
1_40_2	**3.725**	312.6	0.00	3.726	1906.1	0.00	1.000	3.727	303.9	0.00	1.000	3.729	201.7	0.00	1.001
1_40_3	**3.869**	164.3	0.00	3.870	1050.6	0.00	1.000	3.871	245.6	0.00	1.001	3.874	171.6	0.00	1.001
2_40_1	**15.710**	1408.5	0.00	15.712	922.6	0.00	1.000	15.720	397.9	0.01	1.001	15.723	269.9	0.01	1.001
2_40_2	**15.968**	3410.8	0.00	15.970	1520.2	0.00	1.000	15.976	775.8	0.00	1.001	15.984	606.7	0.00	1.001
2_40_3	**15.407**	637.1	0.00	15.409	905.7	0.00	1.000	15.413	257.4	0.00	1.000	15.421	251.2	0.00	1.001
3_40_1	**27.957**	1010.9	0.01	27.979	1452.6	0.00	1.001	27.989	399.8	0.01	1.001	28.047	2741.8	0.01	1.003
3_40_2	**28.151**	574.7	0.00	28.155	981.0	0.00	1.000	28.163	342.7	0.00	1.000	28.168	177.6	0.00	1.001
3_40_3	**27.562**	767.1	0.00	27.577	625.2	0.00	1.001	27.640	207.4	0.00	1.003	27.642	297.5	0.00	1.003
1_50_1	**5.489**	287.7	0.00	5.490	1460.6	0.00	1.000	5.494	337.2	0.01	1.001	5.497	424.4	0.01	1.002
1_50_2	**4.559**	391.2	0.00	4.560	2190.2	0.00	1.000	4.563	419.8	0.00	1.001	4.565	298.8	0.00	1.001
1_50_3	**4.913**	326.9	0.00	**4.913**	1484.5	0.00	1.000	4.915	578.3	0.01	1.001	4.918	391.1	0.01	1.001
2_50_1	**17.367**	2639.8	0.00	17.370	1471.6	0.00	1.000	17.377	508.4	0.01	1.001	17.382	745.4	0.00	1.001
2_50_2	**17.320**	5879.2	0.00	17.323	6528.7	0.00	1.000	17.328	1126.5	0.00	1.000	17.334	431.6	0.01	1.001
2_50_3	**16.566**	2939.8	0.00	16.568	1215.6	0.00	1.000	16.575	624.8	0.00	1.001	16.584	305.7	0.01	1.001
3_50_1	**29.489**	2481.6	0.00	29.494	2792.4	0.00	1.000	29.509	536.3	0.01	1.001	29.520	346.9	0.00	1.001
3_50_2	**29.997**	5671.7	0.00	30.000	1942.1	0.00	1.000	30.009	1021.5	0.00	1.000	30.022	1052.9	0.01	1.001
3_50_3	**29.598**	6965.0	0.00	29.603	3337.3	0.00	1.000	29.611	1269.0	0.00	1.000	29.617	628.1	0.01	1.001
Average	**13.840**	707.8	0.00	13.844	649.1	0.00	1.000	13.853	200.4	0.00	1.001	13.859	190.6	0.01	1.001

Table 10: Performances of PHEV-TSPS-VI and PHEV-TSPSD-VI (Part 2)

Instance	PHEV-TSPS-VI			Speed Discretization											
				0.1 (m/s)				0.3 (m/s)				0.5 (m/s)			
α_β_π	Obj ($\times 10^7$)	$Time$	Gap	Obj_1 ($\times 10^7$)	$Time$	Gap	$\frac{Obj_1}{Obj}$	Obj_2 ($\times 10^7$)	$Time$	Gap	$\frac{Obj_3}{Obj}$	Obj_3 ($\times 10^7$)	$Time$	Gap	$\frac{Obj_3}{Obj}$
1_60_1	**6.557**	3055.0	0.00	6.559	4172.8	0.01	1.000	6.561	1275.3	0.00	1.001	6.570	751.3	0.00	1.002
1_60_2	**5.450**	1446.8	0.00	5.451	4628.0	0.00	1.000	5.454	638.6	0.00	1.001	5.460	924.9	0.01	1.002
1_60_3	**5.902**	7200.2	0.97	5.904	4756.0	0.00	1.000	5.907	1493.9	0.00	1.001	5.910	917.2	0.00	1.001
2_60_1	19.970	7201.3	18.41	**18.977**	4582.8	0.00	0.950	18.983	3569.9	0.00	0.951	18.994	871.3	0.00	0.951
2_60_2	NaN	NaN	NaN	NaN	NaN	NaN	–	**18.656**	7201.0	0.12	–	18.660	698.8	0.01	–
2_60_3	**17.730**	7200.2	3.72	17.733	1810.4	0.01	1.000	17.741	375.1	0.01	1.001	17.745	378.2	0.00	1.001
3_60_1	32.223	7200.2	24.07	**31.249**	5375.6	0.00	0.970	31.264	6070.4	0.01	0.970	31.271	875.8	0.01	0.970
3_60_2	32.655	7200.9	20.76	NaN	NaN	NaN	–	**31.424**	1404.9	0.01	0.962	31.426	1722.2	0.00	0.962
3_60_3	33.552	7200.4	17.88	**31.469**	4984.8	0.00	0.938	31.480	1011.2	0.00	0.938	31.487	1203.6	0.00	0.938
1_70_1	NaN	NaN	NaN	NaN	NaN	NaN	–	**8.181**	3004.6	0.01	–	8.190	1857.8	0.00	–
1_70_2	NaN	NaN	NaN	NaN	NaN	NaN	–	**7.206**	2719.5	0.01	–	7.210	1634.6	0.00	–
1_70_3	6.998	7200.5	1.33	NaN	NaN	NaN	–	**6.986**	3439.5	0.00	0.998	6.991	7202.1	1.12	0.999
2_70_1	NaN	NaN	NaN	NaN	NaN	NaN	–	**21.106**	7201.2	65.97	–	21.118	5842.5	0.01	–
2_70_2	NaN	NaN	NaN	NaN	NaN	NaN	–	**20.087**	7200.5	0.86	–	20.090	1638.0	0.00	–
2_70_3	NaN	NaN	NaN	NaN	NaN	NaN	–	19.415	7203.8	0.64	–	**19.404**	1934.6	0.00	–
3_70_1	NaN	NaN	NaN	NaN	NaN	NaN	–	**32.145**	5562.6	0.00	–	32.152	5426.7	0.01	–
3_70_2	NaN	NaN	NaN	NaN	NaN	NaN	–	**32.804**	1658.5	0.00	–	32.808	3312.3	0.01	–
3_70_3	NaN	NaN	NaN	NaN	NaN	NaN	–	**31.880**	1568.2	0.00	–	31.892	1105.5	0.00	–

[a] The term ‘NaN’ indicates that the instance cannot be solved within 7200 seconds.

Table 11: Comparison of PHEV-TSPS with some other policies

Instance	PHEV-TSPS-VI	Only Fuel Mode		Only Electricity Mode		Sequential Method	
α_β_π	$Obj(\times 10^7)$	$Obj(\times 10^7)$	$Diff$	$Obj(\times 10^7)$	$Diff$	$Obj(\times 10^7)$	$Diff$
1_8_1	**1.602**	3.205	100.00	**1.602**	0.00	**1.602**	0.00
1_8_2	**1.443**	2.886	100.00	**1.443**	0.00	**1.443**	0.00
1_8_3	**1.139**	2.278	100.02	**1.139**	0.00	**1.139**	0.01
2_8_1	**9.707**	12.818	32.05	Inf	Inf	9.751	0.45
2_8_2	**10.269**	13.288	29.41	Inf	Inf	10.357	0.87
2_8_3	**9.844**	12.954	31.59	Inf	Inf	9.849	0.05
3_8_1	**21.698**	24.826	14.42	Inf	Inf	21.703	0.02
3_8_2	**21.930**	25.025	14.11	Inf	Inf	23.243	5.99
3_8_3	**22.038**	25.164	14.18	Inf	Inf	23.585	7.02
1_10_1	**1.814**	3.659	101.70	**1.814**	0.00	1.815	0.05
1_10_2	**1.754**	3.531	101.32	**1.754**	0.00	1.757	0.18
1_10_3	**1.671**	3.354	100.73	**1.671**	0.00	1.674	0.19
2_10_1	**10.132**	13.241	30.68	Inf	Inf	10.138	0.06
2_10_2	**10.438**	13.548	29.80	Inf	Inf	**10.438**	0.00
2_10_3	**10.162**	13.272	30.61	Inf	Inf	10.164	0.03
3_10_1	**21.654**	24.765	14.37	Inf	Inf	23.021	6.31
3_10_2	**21.601**	24.714	14.41	Inf	Inf	21.604	0.01
3_10_3	**22.699**	25.736	13.38	Inf	Inf	24.313	7.11
1_20_1	**2.760**	5.394	95.45	Inf	Inf	2.768	0.30
1_20_2	**2.377**	4.769	100.62	**2.377**	0.00	2.378	0.06
1_20_3	**2.162**	4.353	101.34	**2.162**	0.00	2.166	0.18
2_20_1	**12.934**	16.068	24.23	Inf	Inf	**12.934**	0.00
2_20_2	**12.415**	15.578	25.48	Inf	Inf	12.439	0.19
2_20_3	**12.533**	15.685	25.15	Inf	Inf	12.534	0.00
3_20_1	**24.556**	27.704	12.82	Inf	Inf	24.565	0.04
3_20_2	**24.468**	27.325	11.68	Inf	Inf	24.936	1.91
3_20_3	**24.205**	27.326	12.90	Inf	Inf	24.920	2.95
Average	**11.852**	14.536	47.50	_	_	12.120	1.26

[a] $Diff$: the percentage increase (positive) or decrease (negative) compared to PHEV-TSPS-VI; the term 'Inf' indicates that the instances are infeasible using only electricity.

Table 12: Performance of the PHEV-TSPS with fixed speeds

Instance	PHEV-TSPS-VI	Doppstadt, Koberstein, and Vigo (2016)		Speed limits	
α_β_π	$Obj(\times 10^7)$	$Obj(\times 10^7)$	$Diff$	$Obj(\times 10^7)$	$Diff$
1_8_1	**1.602**	1.622	1.26	2.411	50.44
1_8_2	**1.443**	1.456	0.92	2.251	56.03
1_8_3	**1.139**	1.171	2.80	1.788	57.00
2_8_1	**9.707**	11.993	23.54	14.149	45.76
2_8_2	**10.269**	12.865	25.28	13.899	35.36
2_8_3	**9.844**	12.108	22.99	14.072	42.95
3_8_1	**21.698**	26.257	21.01	27.963	28.87
3_8_2	**21.930**	26.392	20.35	28.357	29.31
3_8_3	**22.038**	26.915	22.13	28.335	28.57
1_10_1	**1.814**	1.860	2.53	2.563	41.28
1_10_2	**1.754**	1.773	1.10	2.387	36.12
1_10_3	**1.671**	1.691	1.21	2.357	41.08
2_10_1	**10.132**	12.319	21.59	14.246	40.60
2_10_2	**10.438**	12.781	22.45	14.374	37.71
2_10_3	**10.162**	12.699	24.97	14.460	42.30
3_10_1	**21.654**	26.372	21.79	28.851	33.24
3_10_2	**21.601**	26.600	23.14	28.091	30.04
3_10_3	**22.699**	27.131	19.53	28.523	25.66
1_20_1	**2.760**	3.973	43.95	4.275	54.90
1_20_2	**2.377**	3.781	59.08	3.783	59.13
1_20_3	**2.162**	2.343	8.38	3.027	40.03
2_20_1	**12.934**	15.364	18.79	16.959	31.12
2_20_2	**12.415**	14.369	15.74	15.764	26.97
2_20_3	**12.533**	14.404	14.93	16.159	28.93
3_20_1	**24.556**	27.767	13.08	30.537	24.36
3_20_2	**24.468**	27.829	13.74	28.850	17.91
3_20_3	**24.205**	27.630	14.15	28.862	19.24
Average	**11.852**	14.128	17.79	15.455	37.22

Table 13: Performance of PHEV-TSPS on different road gradients

Instance	Max Elevation = 100 (m)		Max Elevation = 200 (m)		Max Elevation = 300 (m)		$\frac{Obj_2}{Obj_1}$	$\frac{Obj_3}{Obj_2}$
α_β_π	$Obj_1(\times 10^7)$	$Time$	$Obj_2(\times 10^7)$	$Time$	$Obj_3(\times 10^7)$	$Time$		
1_8_1	**1.602**	0.4	2.265	1.0	2.599	1.7	1.413	1.148
1_8_2	**1.443**	0.5	1.840	0.7	1.973	0.4	1.275	1.072
1_8_3	**1.139**	0.4	1.690	0.1	2.465	0.3	1.484	1.459
2_8_1	**9.707**	1.3	10.574	1.5	10.939	1.4	1.089	1.035
2_8_2	**10.269**	1.8	10.506	1.5	10.575	1.8	1.023	1.007
2_8_3	**9.844**	1.8	11.128	1.9	11.394	1.9	1.130	1.024
3_8_1	21.698	1.7	**21.632**	1.8	21.910	1.4	0.997	1.013
3_8_2	**21.930**	1.6	22.118	1.7	22.208	1.7	1.009	1.004
3_8_3	**22.038**	1.9	22.066	1.8	22.202	1.6	1.001	1.006
1_10_1	**1.814**	0.9	2.429	0.4	3.157	1.4	1.339	1.300
1_10_2	**1.754**	0.6	2.359	1.3	2.191	0.5	1.345	0.929
1_10_3	**1.671**	0.9	1.980	0.6	2.444	0.2	1.185	1.234
2_10_1	**10.132**	2.3	10.620	2.0	10.688	1.5	1.048	1.006
2_10_2	**10.438**	2.0	11.501	2.2	11.428	2.5	1.102	0.994
2_10_3	**10.162**	2.5	11.618	2.7	12.182	2.3	1.143	1.048
3_10_1	**21.654**	2.4	21.680	2.8	22.293	3.0	1.001	1.028
3_10_2	**21.603**	2.7	22.795	2.8	22.516	2.7	1.055	0.988
3_10_3	**22.699**	2.9	23.227	3.0	23.619	2.6	1.023	1.017
1_20_1	**2.760**	14.1	3.277	11.1	4.344	8.6	1.187	1.326
1_20_2	**2.377**	3.5	2.789	8.2	4.173	20.7	1.173	1.496
1_20_3	**2.162**	13.8	2.589	7.4	2.950	6.7	1.198	1.139
2_20_1	**12.934**	31.5	14.277	30.2	14.691	25.5	1.104	1.029
2_20_2	**12.415**	42.4	13.251	30.3	14.033	36.1	1.067	1.059
2_20_3	**12.533**	41.3	13.416	25.3	13.773	26.5	1.070	1.027
3_20_1	**24.556**	34.2	26.166	35.2	26.521	42.2	1.066	1.014
3_20_2	**24.468**	49.7	25.460	47.3	27.465	31.1	1.041	1.079
3_20_3	**24.205**	49.3	25.403	40.5	26.265	19.3	1.050	1.034
Average	**11.852**	10.8	12.543	10.2	13.000	9.1	1.134	1.093

Table 14: Performance of PHEV-TSPS without energy recuperation

Instance	Max Elevation = 100 (m)			Max Elevation = 200 (m)			Max Elevation = 300 (m)		
α_β_π	$Obj_1(\times 10^7)$	$Time$	$Ratio$	$Obj_2(\times 10^7)$	$Time$	$Ratio$	$Obj_3(\times 10^7)$	$Time$	$Ratio$
1_ 8_1	**1.602**	0.6	1.000	2.290	0.3	1.011	2.652	0.5	1.020
1_ 8_2	**1.443**	0.3	1.000	1.840	0.5	1.000	1.992	0.1	1.010
1_ 8_3	**1.139**	0.3	1.000	1.721	0.1	1.018	2.527	0.3	1.025
2_ 8_1	**9.707**	1.1	1.000	10.574	1.7	1.000	10.982	1.3	1.004
2_ 8_2	**10.280**	1.4	1.001	10.507	1.1	1.000	10.575	1.3	1.000
2_ 8_3	**9.844**	1.4	1.000	11.154	1.8	1.002	11.398	1.4	1.000
3_ 8_1	21.716	1.4	1.001	**21.632**	1.1	1.000	21.910	1.3	1.000
3_ 8_2	**21.930**	1.4	1.000	22.118	1.6	1.000	22.227	1.3	1.001
3_ 8_3	**22.060**	2.0	1.001	22.088	1.4	1.001	22.205	1.4	1.000
1_10_1	**1.830**	0.7	1.008	2.449	1.0	1.008	3.230	1.0	1.023
1_10_2	**1.765**	0.6	1.007	2.386	0.9	1.011	2.209	0.1	1.008
1_10_3	**1.677**	0.8	1.004	1.994	0.3	1.007	2.476	0.3	1.013
2_10_1	**10.132**	2.2	1.000	10.624	2.2	1.000	10.703	1.6	1.001
2_10_2	**10.438**	1.9	1.000	11.529	1.8	1.002	11.433	1.6	1.000
2_10_3	**10.162**	2.9	1.000	11.671	2.6	1.005	12.221	2.0	1.003
3_10_1	**21.658**	2.3	1.000	21.708	2.1	1.001	22.335	2.1	1.002
3_10_2	**21.604**	2.7	1.000	22.827	2.1	1.001	22.541	2.5	1.001
3_10_3	**22.704**	2.6	1.000	23.252	2.9	1.001	23.657	2.7	1.002
1_20_1	**2.781**	6.2	1.008	3.304	8.8	1.008	4.435	8.0	1.021
1_20_2	**2.384**	4.1	1.003	2.846	5.4	1.021	4.288	13.4	1.027
1_20_3	**2.177**	4.7	1.007	2.620	4.6	1.012	3.028	4.1	1.026
2_20_1	**12.958**	23.4	1.002	14.299	25.0	1.002	14.784	11.4	1.006
2_20_2	**12.468**	18.1	1.004	13.366	14.7	1.009	14.086	12.7	1.004
2_20_3	**12.575**	20.8	1.003	13.483	16.1	1.005	13.822	26.2	1.004
3_20_1	**24.594**	16.2	1.002	26.225	18.0	1.002	26.655	11.8	1.005
3_20_2	**24.485**	21.3	1.001	25.545	16.8	1.003	27.558	15.8	1.003
3_20_3	**24.226**	21.6	1.001	25.494	11.9	1.004	26.288	12.9	1.001
Average	**11.865**	6.6	1.003	12.576	5.3	1.006	13.045	5.3	1.009

[a] *Ratio* represents the objective values in Table 14 divided by the objective values in Table 13.

Table 15: Impact of charging stations on PHEV-TSPS

Instance	PHEV-TSPS-VI			PHEV-TSPS-CS				PHEV-TSPS-CSwF			
α_β_π	*Obj*	*Time*	*Gap*	*Obj*	*Time*	*Gap*	*Diff*	*Obj*	*Time*	*Gap*	*Diff*
1_8_1	**1.525**	0.1	0.00	**1.525**	0.1	0.00	0.00	**1.525**	0.0	0.00	0.00
1_8_2	**1.392**	0.0	0.00	**1.392**	0.1	0.00	0.00	**1.392**	0.1	0.00	0.00
1_8_3	**1.124**	0.1	0.00	**1.124**	0.1	0.00	0.00	**1.124**	0.0	0.00	0.00
2_8_1	7.789	0.6	0.00	**5.491**	0.5	0.00	-29.51	**5.491**	0.6	0.00	-29.51
2_8_2	7.999	1.1	0.00	**5.613**	1.0	0.00	-29.83	**5.613**	0.5	0.00	-29.83
2_8_3	7.828	0.7	0.00	**5.510**	0.5	0.00	-29.61	**5.510**	0.3	0.00	-29.61
3_8_1	16.709	1.6	0.00	**13.355**	1.8	0.00	-20.07	Inf	Inf	Inf	Inf
3_8_2	16.687	1.7	0.00	**12.359**	1.8	0.00	-25.93	Inf	Inf	Inf	Inf
3_8_3	16.867	1.6	0.00	**11.881**	1.7	0.00	-29.56	Inf	Inf	Inf	Inf
1_10_1	**1.728**	0.2	0.00	**1.728**	0.1	0.00	0.00	**1.728**	0.2	0.00	0.00
1_10_2	**1.700**	0.0	0.00	**1.700**	0.1	0.00	0.00	**1.700**	0.1	0.00	0.00
1_10_3	**1.599**	0.4	0.00	**1.599**	0.3	0.00	0.00	**1.599**	0.3	0.00	0.00
2_10_1	8.071	1.3	0.00	**5.643**	0.8	0.00	-30.08	**5.643**	0.8	0.00	-30.08
2_10_2	8.184	1.8	0.00	**5.687**	0.7	0.00	-30.51	**5.687**	0.9	0.00	-30.51
2_10_3	8.080	1.2	0.00	**5.648**	1.0	0.00	-30.10	**5.648**	1.0	0.00	-30.10
3_10_1	16.785	1.8	0.00	**12.126**	2.5	0.00	-27.75	Inf	Inf	Inf	Inf
3_10_2	16.600	2.6	0.00	**11.829**	2.6	0.00	-28.75	Inf	Inf	Inf	Inf
3_10_3	17.211	2.0	0.00	**12.054**	2.4	0.00	-29.96	Inf	Inf	Inf	Inf
1_20_1	**2.497**	12.5	0.00	**2.497**	8.1	0.00	0.00	**2.497**	5.4	0.00	0.00
1_20_2	**2.246**	2.7	0.00	**2.246**	2.2	0.00	0.00	**2.246**	1.6	0.00	0.00
1_20_3	**2.053**	11.4	0.00	**2.053**	9.8	0.00	0.00	**2.053**	5.8	0.00	0.00
2_20_1	10.194	13.6	0.00	**6.759**	9.9	0.00	-33.69	**6.759**	5.4	0.00	-33.69
2_20_2	9.778	20.3	0.00	**6.530**	9.4	0.00	-33.22	**6.530**	4.7	0.00	-33.22
2_20_3	9.859	16.1	0.00	**6.579**	12.9	0.00	-33.27	**6.579**	10.1	0.00	-33.27
3_20_1	18.810	23.5	0.01	**12.838**	93.2	0.00	-31.75	Inf	Inf	Inf	Inf
3_20_2	18.178	19.4	0.00	**12.864**	34.6	0.00	-29.23	Inf	Inf	Inf	Inf
3_20_3	18.363	16.0	0.00	**12.900**	27.9	0.00	-29.75	Inf	Inf	Inf	Inf
1_30_1	2.776	59.9	0.00	**2.690**	30.1	0.00	-3.08	**2.690**	12.6	0.00	-3.08
1_30_2	**2.285**	17.9	0.00	**2.285**	10.2	0.00	0.00	**2.285**	10.3	0.00	0.00
1_30_3	2.889	81.2	0.01	**2.747**	21.8	0.00	-4.90	**2.747**	19.2	0.00	-4.90
2_30_1	10.743	67.7	0.00	**7.048**	38.2	0.00	-34.39	**7.048**	18.4	0.00	-34.39
2_30_2	10.688	75.9	0.00	**7.017**	46.1	0.00	-34.35	**7.017**	42.9	0.00	-34.35
2_30_3	10.888	174.5	0.00	**7.112**	56.0	0.00	-34.68	**7.112**	71.2	0.00	-34.68
3_30_1	19.979	100.3	0.00	**13.716**	152.6	0.00	-31.35	Inf	Inf	Inf	Inf
3_30_2	19.921	132.8	0.00	**13.563**	183.8	0.00	-31.92	Inf	Inf	Inf	Inf
3_30_3	19.725	160.1	0.00	**13.468**	102.3	0.00	-31.72	Inf	Inf	Inf	Inf
1_40_1	3.717	114.9	0.01	**3.210**	48.2	0.00	-13.64	**3.210**	40.1	0.00	-13.64
1_40_2	3.227	212.0	0.00	**2.926**	99.8	0.00	-9.31	**2.926**	157.3	0.01	-9.31
1_40_3	3.285	152.5	0.00	**2.973**	102.7	0.00	-9.48	**2.973**	87.1	0.00	-9.48
2_40_1	12.022	179.2	0.00	**7.751**	119.6	0.00	-35.53	**7.751**	143.9	0.00	-35.53
2_40_2	12.167	1430.7	0.00	**7.814**	623.7	0.00	-35.78	**7.814**	393.1	0.00	-35.78
2_40_3	11.870	539.1	0.00	**7.644**	256.7	0.00	-35.60	**7.644**	164.4	0.00	-35.60
3_40_1	21.008	313.6	0.00	**14.130**	669.8	0.00	-32.74	Inf	Inf	Inf	Inf
3_40_2	20.911	308.2	0.00	**14.135**	753.2	0.00	-32.40	Inf	Inf	Inf	Inf
3_40_3	20.946	761.1	0.00	**14.177**	7200.2	0.04	-32.32	Inf	Inf	Inf	Inf
1_50_1	4.639	388.1	0.00	**3.741**	414.8	0.00	-19.35	**3.741**	306.3	0.00	-19.35
1_50_2	3.907	627.2	0.00	**3.308**	170.8	0.01	-15.33	**3.308**	176.1	0.00	-15.33
1_50_3	4.172	161.5	0.00	**3.465**	210.5	0.00	-16.96	**3.465**	191.6	0.00	-16.96
2_50_1	13.165	1189.7	0.00	**8.403**	1360.2	0.00	-36.17	**8.403**	732.9	0.00	-36.17
2_50_2	13.283	7200.2	0.28	**8.413**	4251.5	0.00	-36.66	**8.413**	6274.2	0.01	-36.66
2_50_3	12.716	1518.8	0.01	**8.093**	419.5	0.00	-36.36	**8.093**	586.9	0.00	-36.36
3_50_1	22.233	2160.7	0.00	**14.831**	7200.1	0.74	-33.29	Inf	Inf	Inf	Inf
3_50_2	21.981	997.9	0.00	**14.701**	6347.0	0.00	-33.12	Inf	Inf	Inf	Inf
3_50_3	22.091	7200.6	0.41	**14.847**	7200.2	1.05	-32.79	Inf	Inf	Inf	Inf
Average	10.687	490.4	0.01	**7.514**	709.5	0.03	-22.89	_	_	_	_

References

Alba Martínez MA, Cordeau JF, Dell'Amico M, Iori M, 2013 A branch-and-cut algorithm for the double traveling salesman problem with multiple stacks. INFORMS Journal on Computing 25(1):41–55.

Andelmin J, Bartolini E, 2017 An exact algorithm for the green vehicle routing problem. Transportation Science 51(4):1288–1303.

Bahrami S, Nourinejad M, Amirjamshidi G, Roorda MJ, 2020 The plugin hybrid electric vehicle routing problem: A power-management strategy model. Transportation Research Part C: Emerging Technologies 111:318–333.

Barth M, Boriboonsomsin K, 2008 Real-world carbon dioxide impacts of traffic congestion. Transportation Research Record 2058(1):163–171.

Barth M, Younglove T, Scora G, 2005 Development of a heavy-duty diesel modal emissions and fuel consumption model. Tech. rep. UCB-ITS-PRR-2005-1, California PATH Program, Institute of Transportation Studies, University of California at Berkeley.

Baum M, Dibbelt J, Gemsa A, Wagner D, Zündorf T, 2019 Shortest feasible paths with charging stops for battery electric vehicles. Transportation Science 53(6):1627–1655.

Baum M, Dibbelt J, Wagner D, Zündorf T, 2020 Modeling and engineering constrained shortest path algorithms for battery electric vehicles. Transportation Science 54(6):1571–1600.

Bektaş T, Ehmke JF, Psaraftis HN, Puchinger J, 2019 The role of operational research in green freight transportation. European Journal of Operational Research 274(3):807–823.

Bektaş T, Laporte G, 2011 The pollution-routing problem. Transportation Research Part B: Methodological 45(8):1232–1250.

Bruglieri M, Mancini S, Pezzella F, Pisacane O, 2019 A path-based solution approach for the green vehicle routing problem. Computers & Operations Research 103:109–122.

Carlier M, 2022 New registrations of plug-in hybrid electric cars in canada from 2012 to 2021. URL https://www.statista.com/statistics/571990/new-registrations-of-plug-in-hybrid-electric-cars-in-canada/, viewed 16 February 2023.

Caspari A, Fahr S, Mitsos A, 2021 Optimal eco-routing for hybrid vehicles with powertrain model embedded. IEEE Transactions on Intelligent Transportation Systems 23(9):14632–14648.

Cheng C, Adulyasak Y, Rousseau LM, 2020 Drone routing with energy function: Formulation and exact algorithm. Transportation Research Part B: Methodological 139:364–387.

Cordeau JF, Ghiani G, Guerriero E, 2014 Analysis and branch-and-cut algorithm for the time-dependent travelling salesman problem. Transportation Science 48(1):46–58.

Croxton KL, Gendron B, Magnanti TL, 2003 A comparison of mixed-integer programming models for nonconvex piecewise linear cost minimization problems. Management Science 49(9):1268–1273.

Dabia S, Demir E, Woensel TV, 2017 An exact approach for a variant of the pollution-routing problem. Transportation Science 51(2):607–628.

De Nunzio G, Gharbia IB, Sciarretta A, 2021 A general constrained optimization framework for the eco-routing problem: Comparison and analysis of solution strategies for hybrid electric vehicles. Transportation Research Part C: Emerging Technologies 123:102935.

Demir E, Bektaş T, Laporte G, 2012 An adaptive large neighborhood search heuristic for the pollution-routing problem. European Journal of Operational Research 223(2):346–359.

Demir E, Bektaş T, Laporte G, 2014 The bi-objective pollution-routing problem. European Journal of Operational Research 232(3):464–478.

Desaulniers G, Errico F, Irnich S, Schneider M, 2016 Exact algorithms for electric vehicle-routing problems with time windows. Operations Research 64(6):1388–1405.

Doppstadt C, Koberstein A, Vigo D, 2016 The hybrid electric vehicle–traveling salesman problem. European Journal of Operational Research 253(3):825–842.

Doppstadt C, Koberstein A, Vigo D, 2019 The hybrid electric vehicle—traveling salesman problem with time windows instances. Mendeley Dataset, URL https://data.mendeley.com/datasets/9j3tt84hyx/1, viewed 8 March 2023.

Doppstadt C, Koberstein A, Vigo D, 2020 The hybrid electric vehicle—traveling salesman problem with time windows. European Journal of Operational Research 284(2):675–692.

Erdoğan S, Miller-Hooks E, 2012 A green vehicle routing problem. Transportation Research Part E: Logistics and Transportation Review 48(1):100–114.

Florio AM, Absi N, Feillet D, 2021 Routing electric vehicles on congested street networks. Transportation Science 55(1):238–256.

Fukasawa R, He Q, Santos F, Song Y, 2018 A joint vehicle routing and speed optimization problem. INFORMS Journal on Computing 30(4):694–709.

Hellström E, Fröberg A, Nielsen L, 2006 A real-time fuel-optimal cruise controller for heavy trucks using road topography information. 2006 SAE World Congress (Detroit, Michigan).

Huang Y, Zhao L, Van Woensel T, Gross JP, 2017 Time-dependent vehicle routing problem with path flexibility. Transportation Research Part B: Methodological 95:169–195.

Keskin M, Çatay B, 2018 A matheuristic method for the electric vehicle routing problem with time windows and fast chargers. Computers & Operations Research 100:172–188.

Latham FO, 2022 2022 ford escape plug-in hybrid range. URL https://www.lathamfordmotors.com/2022-ford-escape-plug-in-hybrid-range/, viewed 8 January 2023.

Liu H, Miao C, Zhu GG, 2019 Optimal hybrid electric vehicle powertrain control based on route and speed optimization. 2019 IEEE 15th International Conference on Control and Automation (ICCA), 350–355.

Macrina G, Laporte G, Guerriero F, Pugliese LDP, 2019 An energy-efficient green-vehicle routing problem with mixed vehicle fleet, partial battery recharging and time windows. European Journal of Operational Research 276(3):971–982.

Mancini S, 2017 The hybrid vehicle routing problem. Transportation Research Part C: Emerging Technologies 78:1–12.

Murakami K, 2017 A new model and approach to electric and diesel-powered vehicle routing. Transportation Research Part E: Logistics and Transportation Review 107:23–37.

Nasri MI, Bektaş T, Laporte G, 2018 Route and speed optimization for autonomous trucks. Computers & Operations Research 100:89–101.

Nejad MM, Mashayekhy L, Grosu D, Chinnam RB, 2017 Optimal routing for plug-in hybrid electric vehicles. Transportation Science 51(4):1304–1325.

Papadimitriou CH, 1977 The euclidean travelling salesman problem is np-complete. Theoretical Computer Science 4(3):237–244.

Pedregosa F, Varoquaux G, Gramfort A, Michel V, Thirion B, Grisel O, Blondel M, Prettenhofer P, Weiss R, Dubourg V, Vanderplas J, Passos A, Cournapeau D, Brucher M, Perrot M, Duchesnay E, 2011 Scikit-learn: Machine learning in Python. Journal of Machine Learning Research 12:2825–2830.

Pelletier S, Jabali O, Laporte G, 2019 The electric vehicle routing problem with energy consumption uncertainty. Transportation Research Part B: Methodological 126:225–255.

Roberti R, Wen M, 2016 The electric traveling salesman problem with time windows. Transportation Research Part E: Logistics and Transportation Review 89:32–52.

Rocha Y, Subramanian A, 2023 Hybrid genetic search for the traveling salesman problem with hybrid electric vehicle and time windows. Computers & Operations Research 155:106223.

Scora G, Barth M, 2006 Comprehensive modal emissions model (cmem), version 3.01. User guide. Centre for environmental research and technology. University of California, Riverside 1070.

Sioshansi R, 2012 Or forum—modeling the impacts of electricity tariffs on plug-in hybrid electric vehicle charging, costs, and emissions. Operations Research 60(3):506–516.

Stoer M, Wagner F, 1997 A simple min-cut algorithm. Journal of the ACM (JACM) 44(4):585–591.

Sun Z, Zhou X, 2016 To save money or to save time: Intelligent routing design for plug-in hybrid electric vehicle. Transportation Research Part D: Transport and Environment 43:238–250.

UPS, 2022 Electrifying our future. URL https://about.ups.com/us/en/social-impact/environment/sustainable-services/electric-vehicles---about-ups.html, viewed 16 February 2023.

Wu F, Bektaş T, Dong M, Ye H, Zhang D, 2021 Optimal driving for vehicle fuel economy under traffic speed uncertainty. Transportation Research Part B: Methodological 154:175–206.

Yi Z, Bauer PH, 2018 Optimal stochastic eco-routing solutions for electric vehicles. IEEE Transactions on Intelligent Transportation Systems 19(12):3807–3817.

Yi Z, Shirk M, 2018 Data-driven optimal charging decision making for connected and automated electric vehicles: A personal usage scenario. Transportation Research Part C: Emerging Technologies 86:37–58.

Yi Z, Smart J, Shirk M, 2018 Energy impact evaluation for eco-routing and charging of autonomous electric vehicle fleet: Ambient temperature consideration. Transportation Research Part C: Emerging Technologies 89:344–363.